The Journal of Physiology

Biophysical Modelling of Intrinsic Cardiac Nervous System Neuronal Electrophysiology based on Single-cell Transcriptomics

Suranjana Gupta, Michelle M Gee, Adam John Hunter Newton, Lakshmi Kuttippurathu, Alison Moss, John D. Tompkins, James S Schwaber, Rajanikanth Vadigepalli, and William Lytton
DOI: 10.1113/JP287595

Corresponding author(s): Rajanikanth Vadigepalli (Rajanikanth.Vadigepalli@jefferson.edu)

The referees have opted to remain anonymous.

Review Timeline:

Submission Date:	30-Aug-2024
Editorial Decision:	12-Nov-2024
Revision Received:	31-Dec-2024
Accepted:	14-Feb-2025

Senior Editor: Natalia Trayanova

Reviewing Editor: Eleonora Grandi

Transaction Report:

(Note: With the exception of the correction of typographical or spelling errors that could be a source of ambiguity, letters and reports are not edited. Depending on transfer agreements, referee reports obtained elsewhere may or may not be included in this compilation. Referee reports are anonymous unless the Referee chooses to sign their reports.)

Dear Dr Vadigepalli,

Re: JP-RP-2024-287595 "Biophysical Modelling of Intrinsic Cardiac Nervous System Neuronal Electrophysiology based on Single-cell Transcriptomics" by Suranjana Gupta, Michelle M Gee, Adam Newton, Lakshmi Kuttippurathu, Alison Moss, John D. Tompkins, James S Schwaber, Rajanikanth Vadigepalli, and William Lytton

Thank you for submitting your manuscript to The Journal of Physiology. It has been assessed by a Reviewing Editor and by 1 expert referees and we are pleased to tell you that it is potentially acceptable for publication following satisfactory major revision.

Please advise your co-authors of this decision as soon as possible.

The referee reports are copied at the end of this email.

Please address all the points raised and incorporate all requested revisions or explain in your Response to Referees why a change has not been made. We hope you will find the comments helpful and that you will be able to return your revised manuscript within 9 months. If you require longer than this, please contact journal staff: jp@physoc.org. Please note that this letter does not constitute a guarantee for acceptance of your revised manuscript.

Your revised manuscript should be submitted online using the link in your Author Tasks: Link Not Available. This link is accessible via your account as Corresponding Author; it is not available to your co-authors. If this presents a problem, please contact journal staff (jp@physoc.org). Image files from the previous version are retained on the system. Please ensure you replace or remove any files that are being revised.

If you do not wish to submit a revised version of your manuscript, you must inform our journal staff (jp@physoc.org) or reply to this email to request withdrawal. Please note that a manuscript must be formally withdrawn from the peer review process at one journal before it may be submitted to another journal.

TRANSPARENT PEER REVIEW POLICY: To improve the transparency of its peer review process, The Journal of Physiology publishes online as supporting information the peer review history of all articles accepted for publication. Readers will have access to decision letters, including Editors' comments and referee reports, for each version of the manuscript, as well as any author responses to peer review comments. Referees can decide whether or not they wish to be named on the peer review history document.

ABSTRACT FIGURES: Authors are expected to use The Journal's premium BioRender account to create/redraw their Abstract Figures. Information on how to access this account is here: https://physoc.onlinelibrary.wiley.com/journal/14697793/biorender-access.

This will enable Authors to create and download high-resolution figures. If authors have used the free BioRender service, they can use the instructions provided in the link above to download a high-resolution version suitable for publication.

The link provided should only be used for the purposes of this submission. Authors will be charged for figures created on this account if they are not related to this manuscript submission.

LANGUAGE EDITING AND SUPPORT FOR PUBLICATION: If you would like help with English language editing, or other article preparation support, Wiley Editing Services offers expert help, including English Language Editing, as well as translation, manuscript formatting, and figure formatting at www.wileyauthors.com/eeo/preparation. You can also find resources for Preparing Your Article for general guidance about writing and preparing your manuscript at www.wileyauthors.com/eeo/prepresources.

RIGOUR AND REPRODUCIBILITY: We recommend authors consult The Journal's Rigour and Reproducibility requirements to ensure that their manuscript is suitable for publication: https://physoc.onlinelibrary.wiley.com/pb-assets/hub-assets/physoc/documents/TJP-Rigour-and-Reproducibility-Requirements.pdf

REVISION CHECKLIST:

Check that your Methods section conforms to journal policy: https://jp.msubmit.net/cgi-bin/main.plex?form_type=display_requirements#methods.

Check that data presented conforms to the statistics policy: https://jp.msubmit.net/cgi-bin/main.plex?form_type=display_requirements#statistics.

Upload a full Response to Referees file. To create your 'Response to Referees': copy all the reports, including any comments from the Senior and Reviewing Editors, into a Microsoft Word, or similar, file and respond to each point, using font or background colour to distinguish comments and responses and upload as the required file type.

Please upload two versions of your manuscript text: one with all relevant changes highlighted and one clean version with no changes tracked. The manuscript file should include all tables and figure legends, but each figure/graph should be uploaded as separate, high-resolution files.

You may also upload:

- 'Potential Cover Art' for consideration as the issue's cover image
- Appropriate Supporting Information (Video, audio or data set: see https://jp.msubmit.net/cgi-bin/main.plex?form_type=display_requirements#supp).

We look forward to receiving your revised submission.

If you have any queries, please reply to this email and we will be pleased to advise.

Yours sincerely,

Natalia Trayanova
Senior Editor
The Journal of Physiology

Reviewing Editor's comments:

Apologies for the late review. One reviewer did not return their assessment and stopped responding to our email.

The reviewer finds the aim of this study to be of interest, but points out a number of concerns regarding the approach - including the model of choice for this study. The authors are also invited to provide experimental evidence for their assumptions or accepted parameter combinations. Please note a marked up PDF is available in addition to the summary or critiques.

Referee #2:

The study is motivated by a fascinating idea, which is, being able to explicitly include information about patterns of ion channel expression into an excitable membrane model, in this case, from intrinsic cardiac neuron transcriptomics. However, the models were chosen from databases that assume channel dynamics, in particular gating dynamics, that by their formulation bias the predictions in at least a couple of ways. The most important one is the use of powers in the gating terms, which impact the sizes of the maximal conductances of the model. One key question that arises from this is: are the ratios of Na and K maximal conductances equivalent to the ratios of the levels of expression from the data corresponding to Na and K channels? The models chosen for the study, as presented, predict ratios of 3-5 times as many Nav1.1 channels as

Kv1.1 channels, for instance. Is this accurate? I would very much like to see some evidence to that effect. Electrophysiological recordings and other splice variant data indicate the opposite (several fold more K channels in comparison to Na channels, for instance), but that is not conclusive data that applies to all species and neurons within them.

Regarding originality, the question has been asked before (e.g. Herrera-Valdez, et al. 2013, Nowotny et al. 2007), but to my knowledge, there have not been any studies in which transcriptomic or proteomic data have been used. In this regard, the study is motivated by a very interesting paradigm linking modelling and experimental measurements, but again, choose arbitrarily from model databases arguing that many people use those models (see comments about powers in gating terms in annotated pdfs and above). One important fact to consider is that the behaviour of the neurons of interest in the study can be captured initially with a simple 2D model with voltage-gated Na and K-delayed rectifier channels. The conclusions from using a model with high dimensionality are hard to interpret and it is easy to conclude, wrongly, that "wild combinations of parameters indicate wild combinations of expression levels", as suggested by some. Highly dimensional models may show combinations of parameters that may not be correct in light of physiological considerations. Also, the authors choose to model ionic currents with different functional forms (fundamentally different assumptions for the underlying biophysics) within the same model, which does not help for interpretation.

As to the dynamics of the model, since there seems to be a gradient of behaviours that stem all from phenomena captured by 2D biophysics, I think the authors could have focused on building up from simple models to tackle the issues of diversity in the neuronal population, to network dynamics as mentioned in the discussion of the paper. The model does not go significantly further in making predictions, in comparison to the transcriptomics data, but analysing the dynamics from a tractable perspective would have been more informative, and then the inclusion of more ion channels to explain how redundancies occur would have been appropriate.

In spite of the poor modelling and choices, and having done no geometrical or other kinds of analysis that are more meaningful than the statistics, I believe that the approach heads fundamentally in the right direction, and other modelling approaches could complement what is reported in this study, provided that the transcriptomic data is shared properly (not just the binary data about whether a channel gene is transcribed or not).

END OF COMMENTS

The Journal of Physiology

https://jp.msubmit.net

JP-RP-2024-287595

Title: Biophysical Modelling of Intrinsic Cardiac Nervous System Neuronal Electrophysiology based on Single-cell Transcriptomics

Authors: Suranjana Gupta
Michelle Gee
Adam Newton
Lakshmi Kuttippurathu
Alison Moss
John Tompkins
James Schwaber
Rajanikanth Vadigepalli
William Lytton

Author Conflict: No competing interests declared

Author Contribution: Suranjana Gupta: Acquisition, analysis or interpretation of data for the work; Drafting the work or revising it critically for important intellectual content; Final approval of the version to be published; Agreement to be accountable for all aspects of the work Michelle Gee: Acquisition, analysis or interpretation of data for the work; Drafting the work or revising it critically for important intellectual content; Final approval of the version to be published; Agreement to be accountable for all aspects of the work Adam Newton: Acquisition, analysis or

interpretation of data for the work; Drafting the work or revising it critically for important intellectual content; Final approval of the version to be published; Agreement to be accountable for all aspects of the work Lakshmi Kuttippurathu: Acquisition, analysis or interpretation of data for the work; Drafting the work or revising it critically for important intellectual content; Final approval of the version to be published; Agreement to be accountable for all aspects of the work Alison Moss: Acquisition, analysis or interpretation of data for the work; Drafting the work or revising it critically for important intellectual content; Final approval of the version to be published; Agreement to be accountable for all aspects of the work John Tompkins: Acquisition, analysis or interpretation of data for the work; Drafting the work or revising it critically for important intellectual content; Final approval of the version to be published; Agreement to be accountable for all aspects of the work James Schwaber: Conception or design of the work; Drafting the work or revising it critically for important intellectual content; Final approval of the version to be published; Agreement to be accountable for all aspects of the work Rajanikanth Vadigepalli: Conception or design of the work; Acquisition, analysis or interpretation of data for the work; Drafting the work or revising it critically for important intellectual content; Final approval of the version to be published; Agreement to be accountable for all aspects of the work William Lytton: Acquisition, analysis or interpretation of data for the work; Drafting the work or revising it critically for important intellectual content; Final approval of the version to be published; Agreement to be accountable for all aspects of the work

Running Title: Biophysical Modeling of Intrinsic Cardiac Neurons

Dual Publication: No

Funding: HHS | NIH | National Heart, Lung, and Blood Institute (NHLBI): James S Schwaber, Rajanikanth Vadigepalli, U01 HL133360; HHS | NIH | National Heart, Lung, and Blood Institute (NHLBI): James S Schwaber, Rajanikanth Vadigepalli, R01 HL161696; HHS | NIH | NIH Office of the Director (OD): Rajanikanth Vadigepalli, OT2 OD030534

Biophysical Modelling of Intrinsic Cardiac Nervous System Neuronal Electrophysiology based on Single-cell Transcriptomics

Suranjana Gupta[1,†], Michelle M. Gee[2,3,†], Adam J.H. Newton[1], Lakshmi Kuttippurathu[2], Alison Moss[2], John D. Tompkins[4], James S. Schwaber[2,3], Rajanikanth Vadigepalli[2,3,*], and William W. Lytton[1,5]

[1]*Department of Physiology and Pharmacology, SUNY Downstate Health Sciences University, Brooklyn, NY, USA*

[2]*Daniel Baugh Institute for Functional Genomics/Computational Biology, Department of Pathology and Genomic Medicine, Thomas Jefferson University, Philadelphia, PA, USA*

[3]*Department of Chemical and Biomolecular Engineering, University of Delaware, Newark, DE, USA*

[4]*Department of Medicine, Cardiac Arrhythmia Center and Neurocardiology Research Program of Excellence, University of California, Los Angeles, CA, USA*

[5]*Department of Neurology, Kings County Hospital, Brooklyn, NY, US*

*Corresponding author: Rajanikanth Vadigepalli, Rajanikanth.Vadigepalli@jefferson.edu

[†]Co-first author

Abstract

The intrinsic cardiac nervous system (ICNS), termed as the heart's "little brain", is the final point of neural regulation of cardiac function. Studying the dynamic behaviour of these ICNS neurons via multiscale neuronal computer models has been limited by the sparsity of electrophysiological data. We developed and analysed a computational library of neuronal electrophysiological models based on single neuron transcriptomics data obtained from ICNS neurons. Each neuronal phenotype was characterized by a unique combination of ion channels identified from the transcriptomic data, using a cycle threshold cutoff that ensured electrical excitability of the neuronal models. The parameters of the ion channel models were grounded based on passive properties: resting membrane potential, input impedance, and rheobase. Consistent with experimental observations, the emergent model dynamics showed phasic activity in response to current clamp stimulus in a majority of neuronal phenotypes (61%). Additionally, 24% of the ICNS neurons showed tonic response, 11% were phasic-to-tonic with increasing current stimulation, and 3% showed tonic-to-phasic behaviour. The computational approach and the library of models bridge the gap between widely available molecular-level gene expression and sparse cellular-level electrophysiology for studying the functional role of the ICNS in cardiac regulation and pathology.

Key points

- We developed computational models of neuron electrophysiology from single-cell transcriptomics data from neurons in the heart's "little brain": the intrinsic cardiac nervous system.
- The single-cell transcriptomic data formed the basis for ion channel combinations in each neuronal model.
- The library of neuronal models was constrained by the passive electrical properties of the neurons and predicts a distribution of phasic and tonic responses that aligns with experimental observations.
- Heterogeneity in the electrophysiological behavior of neurons is driven by variation in ion channel expression.
- These neuron models are a first step towards connecting single-cell transcriptomics data to dynamic, predictive physiology-based models.

Introduction

Parasympathetic and sympathetic imbalance contributes to the etiology of many cardiovascular diseases. A key regulator of sympathovagal balance is the heart's "little brain", the intrinsic cardiac nervous system (ICNS), which contains both cholinergic and catecholaminergic neurons (J. A. Armour, 2008; Hadaya & Ardell, 2020; Hanna et al., 2021; Moss et al., 2021). As the final neural regulatory point for the heart, the ICNS mediates the balance of parasympathetic and sympathetic inputs to the cardiac tissue. Neural remodelling within ICNS has been linked to the progression of cardiovascular disease (Beaumont et al., 2016; Salavatian et al., 2016; Vaseghi et al., 2017). Both phasic and tonic firing responses have been observed in mouse, pig, and human, and neural remodelling to modulate these behaviors could regulate sympathovagal balance in health and disease (Tompkins et al., 2024).

Phasic and tonic electrophysiological behavior arises from a multitude of ion channel combinations through a complex mapping relating variable molecular expression to relative more constrained functional responses. Recently, the increased availability of high-throughput, single-neuron transcriptomics has made it possible to identify the exact combinations of ion channels present in each cell to connect subcellular components to cellular function (Moss et al., 2021). These transcriptomic datasets have been mined to address questions of how ion channel degeneracy contributes to firing robustness in neurons (Drion et al., 2015; Goaillard & Marder, 2021; Nandi et al., 2022; Roy & Narayanan, 2023), but have not been used to study how high-dimensional ion channel expression collapses to a restricted set of phasic and tonic responsive phenotypes. Differences in ion channel conductances that drive transitions from phasic to tonic firing in a neuron are potential regulatory points for controlling sympathovagal balance in the ICNS.

To address this question, we use the well-established Hodgkin-Huxley models and combine them with single-cell transcriptomics data to identify specific ion channel combinations for each neuron. This computational approach allows us to explore the contributions of individual ion channels that would not be possible without inferring channel involvement through time-consuming pharmacological blockades or assuming channel types (Schwaber et al., 1993; Shevtsova et al., 2020). Instead, *in-*

silico screening can be performed to identify the most important ion channels for further experimental testing. In addition, neurons of the same cell type have electrophysiological behavior consistent with each other in response to current clamp stimulus, but vary in their ion channel conductance densities. This heterogeneity may contribute to the variable responses of neurons of the same type to perturbations, muddling the association between an ion channel and a particular function identified via conventional experimental approaches (Goaillard & Marder, 2021). Electrophysiological recording of neuronal electrical activity has been a productive approach to studying the ICNS to capture neuronal firing rate and membrane electrical behavior, but it is labor-intensive and, therefore, low throughput. More recently, the systems biology approach provides a complementary approach by capitalizing on high-throughput transcriptomic techniques (Hanna et al., 2021; Moss et al., 2021) that are becoming increasingly available through data sharing initiatives, such as the National Institutes of Health's SPARC program (https://sparc.science/).

In this work, we aim to connect the electrophysiological behavior of ICNS neurons to their gene expression using transcriptomics-based single-cell parallel conductance Hodgkin-Huxley neuronal phenotype computational models. We present a strategy for using single-neuron transcriptomic data to predict neuronal membrane physiology, demonstrating a workflow for building a library of neuronal phenotype models. We used data from 321 porcine RAGP neurons to deduce the presence or absence of particular channel types in each neuron. We then used Hodgkin-Huxley ion-channel models from open-source model repositories to construct a library of parallel-conductance models reflecting ion channel combinations and predicting electrophysiological behavior.

Materials and Methods

We propose a 6-step workflow for the development of electrophysiological neuronal models from single-neuron transcriptomics data (Figure 1). We expand upon Steps I and V in Section 2.1, Step III in Section 2.2, and Step IV in Section 2.3.

Morphology, physiology, and transcriptomics of neurons

The morphology of Yucatán minipig RAGP principal neurons (PN) was obtained from previously reported experimental data (Hanna et al., 2021). Porcine RAGP PN somata are generally elliptical with a radius spanning 15 – 30 μm along their minor axis and 20 – 47 μm along their major axis (Hanna et al., 2021; Moss et al., 2021). The typical minipig RAGP neuron cross-sectional area is ~1400 μm^2 and ranges from 600 – 4000 μm^2 (Hanna et al., 2021). In our single-neuron models, we used a 21 μm diameter and 21 μm length to achieve this area using the NEURON software's cylindrical section (Carnevale & Hines, 2006).

Neuronal models of RAGP PN were constrained on the basis of passive electrical properties reported for Yucatán minipig (Hanna et al., 2021), guinea pig (Edwards et al., 1995), rat (Selyanko, 1992), and mouse ICNS (Harper & Adams, 2021; Lizot et al., 2022). These properties were: **1.** resting membrane potential (RMP) near -60 mV (Hanna et al., 2021); **2.** input impedance (R_{in}) 40 – 300 MΩ (Edwards et al., 1995; Hanna et al., 2021; Harper & Adams, 2021; Selyanko, 1992); **3.** rheobase 0.02 – 0.08 nA (Lizot et al., 2022); and **4.** leak reversal potential (E_{pas}) of -80 – -50 mV, corresponding to a range between E_K and E_h.

Previously published HT-qPCR (High Throughput quantitative Polymerase Chain Reaction) data from 405 single RAGP neurons and 15 mRNA transcripts coding for 14 ion channel genes were used to select ion channel presence or absence in single-neuron models (Moss et al., 2021). Each mRNA transcript codes for one ion channel or ion channel subunit. The co-expression of the transcripts *Kcna1* and its subunit *ab1* were translated into equivalent biophysics, as expanded in the subsequent section. Samples were collected from two male and two female Yucatán minipigs using laser capture microdissection (Moss et al., 2021). After examination of the dataset for quality control based on the presence of Na^+ channel expression, samples from one female pig were removed, leaving samples from 321 neurons.

Owing to a gradient in ion channel gene expression, we binarized the data to identify ion channels to include in each neuronal model (Figure 2). A cycle threshold (C_t), which is inversely correlated to gene expression level, was selected as the threshold metric and a value of 15 cycles was found to be a suitable cut-off. Analysis of the effect of C_t threshold on the distribution of neuronal phenotypes and on the electrophysiological behavior in our population of neuronal phenotype models was assessed to justify the selection of 15 as a C_t threshold (**Error! Reference source not found.**). Varying the C_t threshold from 13 – 17 caused new neuronal phenotypes to appear (Figure S1). However, these neuronal phenotypes accounted for only 11 – 21% of the neurons sampled. Neuronal phenotypes 23 and 91 had 10 or more occurrences for four of five C_t thresholds and neuronal phenotypes 4, 30, and 73 were common at three of five C_t thresholds (Figure S2). These results suggest that the majority of cells have common neuronal phenotypes that are robust to C_t threshold changes. The change in neuronal phenotypes also did not alter the distribution of electrophysiological behavior for C_t thresholds of 13 – 16 (**Error! Reference source not found.**). After thresholding with our selected C_t threshold of 15, we identified 104 unique combinations of ion channels from the 321 single-neurons. We refer to each unique combination of ion channels as a *neuronal phenotype*.

Ion channel model selection

Ion channel models for each of the 14 ion channels were selected from three public databases: Channelpedia (channelpedia.epfl.ch; (Ranjan et al., 2011)), ModelDB (modeldb.science; (McDougal et al., 2017)), and Ion Channel Genealogy (icg.neurotheory.ox.ac.uk; (Podlaski et al., 2017)). An in-house library of ion channel models mined from the public databases and literature survey was used to track ion channel model properties, physiological function, experimental protocol, and tissues/cells for model creation. We employed the database to establish provenance and to compare each ion channel isoform model against its counterparts. The initial selection of ion channel models from the databases relied on identifying the extent to which the model could be assigned to a particular gene rather than being a generic model. We used Hodgkin-Huxley parallel conductance models with conductance values for Na^+, K^+, and HCN ion channels (Table 2, Table S1). Calcium channels

used the Goldman–Hodgkin–Katz flux equation with a Maclaurin series expansion of the voltage-dependent terms for numerical stability (Hille, 1992).

We simulated channel combinations to find an ion channel model for each gene that worked in the full parallel-conductance model. The choice of a suitable sodium (*Scn1a*, Nav1.1) channel is particularly important due to its role in spiking. Multiple kinetic models were available, even within a single database. We identified five potential Nav1.1 models (Channelpedia ID #35, ModelDB Accession #20756, #256632, #264834 and Na^+ model reported in (Rybak et al., 1997). We ran comparative simulations to find one model for each ion channel that yielded physiologically stable responses across a range of conductance values. The criteria for selection included E_{pas}, R_{in}, and rheobase within the range of experimentally measured data (Edwards et al., 1995; Hanna et al., 2021; Harper & Adams, 2021; Selyanko, 1992). Three of the five models identified were not suitable, usually due to a large window current which required an unphysiologically large E_{pas} to compensate for the current at rest, or a large R_{in} that produced a very leaky cell. To choose between the remaining two models, we then assessed the rheobase. Various experimental studies have noted a rheobase near 100 pA (Edwards et al., 1995; Hanna et al., 2021; Harper & Adams, 2021; Selyanko, 1992). Comparison of the two Na^+ channel candidates in the full parallel conductance model identified Channelpedia ID #35 as a better fit (Figure S3).

Potassium channel selection was also important for ensuring the possibility of neuronal excitability. *Kcna1* (Kv 1.1) is a delayed rectifier potassium (KDR) channel, which is non- or slowly-inactivating (timescale of seconds) (Song, 2002). Our data set showed robust expression of *Kcna1* (α subunit of Kv 1.1). There was also a dominant expression of *Kcnab1* (β1 regulatory subunit) across all neuronal phenotypes. The subunit *Kcnab1* has been reported to confer fast inactivation in these channels (Allen et al., 2020; Heinemann et al., 1996; Rettig et al., 1994; Sewing et al., 1996). To account for the electrophysiological effect of the β1 subunit, a fast inactivation variable was introduced to our selected *Kcna1* KDR model (ModelDB Accession #80769). The model for *Kcnc1* (Kv 3.1), the most expressed potassium channel gene (Figure 3), was adapted from (Rothman & Manis, 2003a, 2003b, 2003c). The ion channel was fit to a two-component model with fast and slow

activation processes, the relative contribution of which was established by a fractional amplitude parameter (ϕ).

Parameter estimation

Once the ion channel models were chosen, simulations were performed for each ion channel to narrow the range of conductances so that the ensemble model's behavior was physiologically stable. Ion channel conductances were initialized to their default values that came from either an original voltage clamp study in foreign tissue or a published ion channel model. A range of conductances around the default values for each ion channel model was set. Maximal conductance values were constrained sequentially in the order of Na^+, K^+ (*Kcna1*, *Kcnc1*, *Kcnj3*), Ca^{2+} (a, b, c, d, g, i), and HCN (1, 2, 3, 4) channels. This order was selected based on which ion channels are known to contribute most significantly to electrophysiological behavior.

A randomly sampled conductance matrix was chosen from the conductance ranges of respective ion channel models. Preliminary simulations were run to evaluate their passive properties. Combinations of conductances that did not yield physiologically tenable RMPs, R_{in} and rheobase, were rejected. After the stable range for each conductance value was identified, we randomly sampled within this range to produce six models. From six models, we identified three degenerate parameter sets with input impedance (R_{in}), reversal potential (E_{pas}), and rheobase within experimentally observed ranges (Edwards et al., 1995; Hanna et al., 2021; McAllen et al., 2011).

Channel conductances were primarily constrained by the passive electrical properties of the neurons. We had an additional degree of freedom in the fractional amplitude parameter(ϕ_{Kcnc1}), which represents the relative contributions of the fast and slow activation processes in the *Kcnc1* channel. We observed this parameter to mainly control the firing rates (Figure S4). We varied ϕ_{Kcnc1} over a range of stimulus currents, and settled on a value that restricted the firing rates in accordance with experimental data (Harper & Adams, 2021; Vaseghi et al., 2017).

Simulations were run using the three degenerate parameter sets identified. Additional tuning of the channel conductances were required in cases where ensemble models were dominated by artificial firing patterns. These patterns included continued firing without the application of a stimulus, sustained firing activity

post removal of the stimulus and incomplete repolarization resulting in elevated RMP for prolonged periods of time.

Table 1: Model parameters from literature

Parameter	Value	Parameter	Value
Simulation Time	1000 ms	Time Step (*dt*)	25 µs
V_{rmp}	–61 mV	Membrane Threshold	–10 mV
Soma Length	21 µm	Soma Diameter	21 µm
C_m	1 µF/cm^2	R_a	35.4 Ω-cm
No. of segements (*nseg*)	1	Temperature	35ºC
E_{Na}	50 mV	E_K	–77 mV
E_h	–45 mV		

Table 2: Estimated model parameters

Parameter	Value	Literature Model Value
$\overline{g_{Kcnj3}}$	3.5e^{-3} S/cm^2	1e^{-3} S/cm^2
$\overline{g_{Kcna1+ab1}}$	0.018 S/cm^2	0.011 S/cm^2
$\overline{g_{Kcnc1}}$	0.018 S/cm^2	0.011 S/cm^2
ϕ_{Kcnc1}	0.2	0.85
$\overline{g_{Cacna1a}}$	0.00005 S/cm^2	1e^{-5} S/cm^2
$\overline{g_{Cacna1b}}$	0.0001 S/cm^2	1e^{-5} S/cm^2
$\overline{g_{Cacna1c}}$	0.006 S/cm^2	1e^{-5} S/cm^2
$\overline{g_{Cacna1d}}$	0.00045 S/cm^2	1.7e^{-6} S/cm^2
$\overline{g_{Cacna1g}}$	0.0003 S/cm^2	1e^{-5} S/cm^2
$\overline{g_{Cacna1\iota}}$	0.0006 S/cm^2	2e^{-4} S/cm^2
$\overline{g_{HCN1}}$	0.003 S/cm^2	1e^{-5} S/cm^2
$\overline{g_{HCN2}}$	0.009 S/cm^2	1e^{-5} S/cm^2
$\overline{g_{HCN3}}$	0.01 S/cm^2	1e^{-5} S/cm^2
$\overline{g_{HCN4}}$	0.0035 S/cm^2	1e^{-5} S/cm^2
$\overline{g_{Scn1a}}$	0.075 S/cm^2	1e^{-5} S/cm^2

Classically, physiological arrest mechanisms exist to establish reliable operation of the cells' electrical machinery. This ensures the operating points to always be stable. This naturally embedded property needed to be explicitly modeled in our framework and was done via additional tuning of channel conductances. In this paper, we report a single parameter set that was most similar to the experimentally observed electrophysiological behavior (Table 1 and Table 2).

Sensitivity Analysis

Different ion channels underlie different phases of the firing activity such as its duration, inter-spike interval, extent of depolarization and repolarization. The impact of these channels on the above features was assessed by running a sensitivity analysis on the following metrics: firing frequency, AP peak, negative peak of hyperpolarization, and full width at half maximum (FWHM). For a fixed current stimulus of 0.1 nA, the conductance of each channel was incrementally varied with respect to its nominal value (Table 2). For the range of conductances explored, best-fit linear regression curves were fitted wherein the slope best approximated the overall trend of the data, thereby capturing the dependency of the metrics on each ion channel model.

Modelling and simulation tools

The model was implemented using NEURON v8.0 (http://neuron.yale.edu/) and the NetPyNE v1.0.0.2 Sobol branch (http://netpyne.org/) (Dura-Bernal et al., 2019). These modelling tools facilitated parallel simulations on high-performance computing platforms, allowing us to run over 400,000 simulations during model development.

Data and code availability

The model source and analysis code were developed as part of the Stimulating Peripheral Activity to Relieve Conditions (SPARC) program is available on GitHub (https://github.com/Daniel-Baugh-Institute/BiophysicalModellingOfIntrinsicCardiacNeurons) and the SPARC portal (https://doi.org/10.26275/cy9w-ttjn) under a CC-BY 4.0 license. Model source code is also available through ModelDB (https://modeldb.science/2014824). The model can

also be accessed through the simulation platform oSPARC (https://osparc.io/), which enables users to run simulations with the model using a Graphical User Interface. The Ten Simple Rules for the Credible Practice of Modelling and Simulation in Healthcare (Erdemir et al., 2020; Mulugeta et al., 2018) were documented to ensure data availability and can be found in the Supplementary Material.

Results

The model development workflow builds on ion channel expression data along with public resources on ion channel kinetics towards developing integrated electrophysiology models of ICNS neurons (Figure 1). HT-qPCR data from single neurons on ion channel genes were used to select ion channel presence or absence in single-neuron models (Step I) (Moss et al., 2021). The data were binarized to represent ion channel presence or absence using a cycle threshold (C_t) cutoff (Figure 2). Several values for the C_t threshold were considered ranging from 13–17, but a threshold of 15 cycles was selected so that each neuron included voltage-gated sodium channels and at least one voltage-gated potassium channel to ensure the potential for electrical excitability (Edwards et al., 1995; McAllen et al., 2011). Redundant neurons with the same ion channel combinations were removed to identify unique neuronal phenotypes (Step II). Corresponding ion channel models were identified from public databases (Step III). Fixed conductance values were selected for each (Step IV). Known morphological properties of RAGP neurons were incorporated to construct a library of parallel conductance models (Step V). Finally, the model responses to current clamp stimulus were simulated and the firing properties of each neuronal phenotype were analyzed and classified (Step VI).

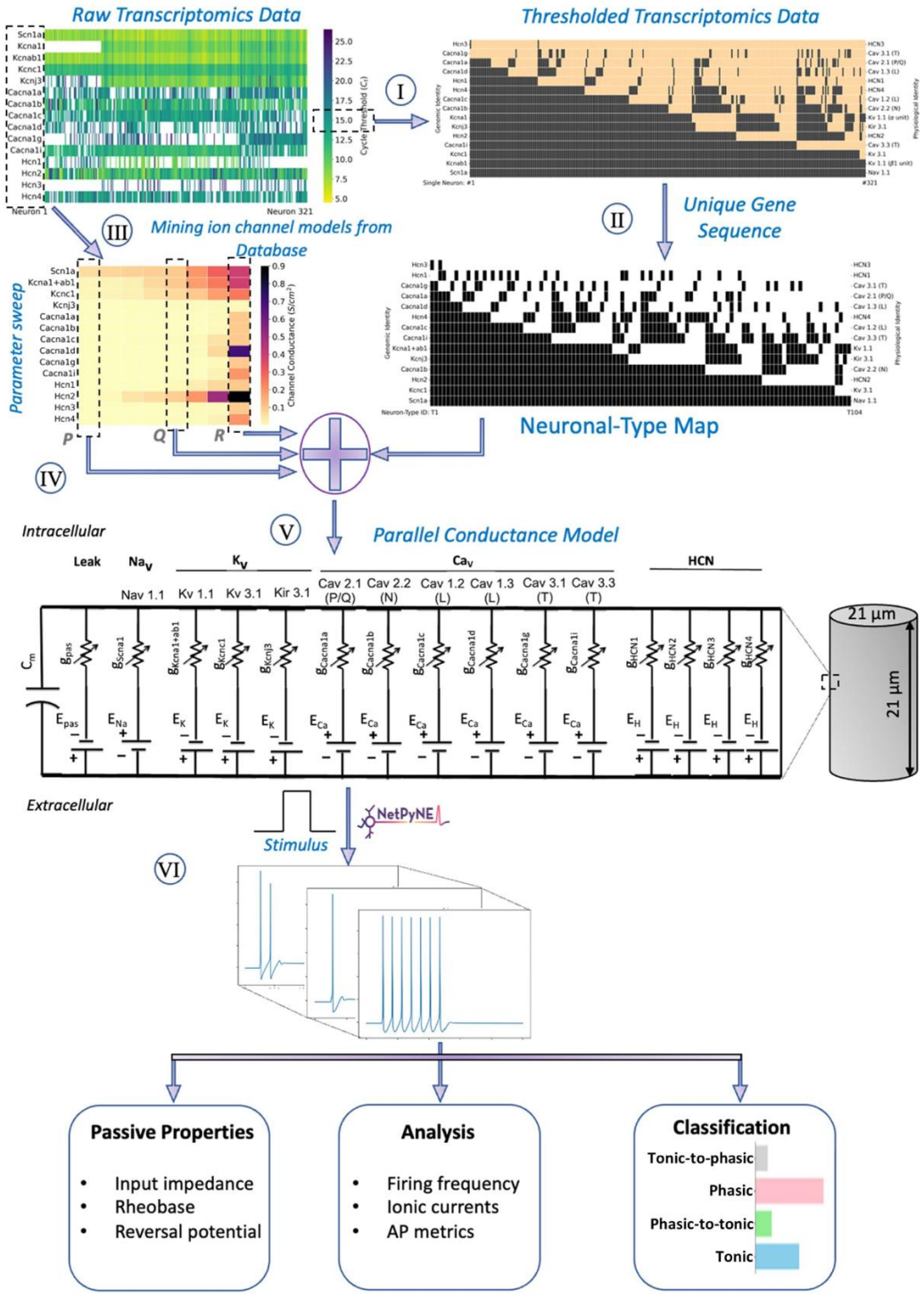

Figure 1: Workflow for development of electrophysiological models starting with single neuron gene expression data and model database of ion channel kinetics.

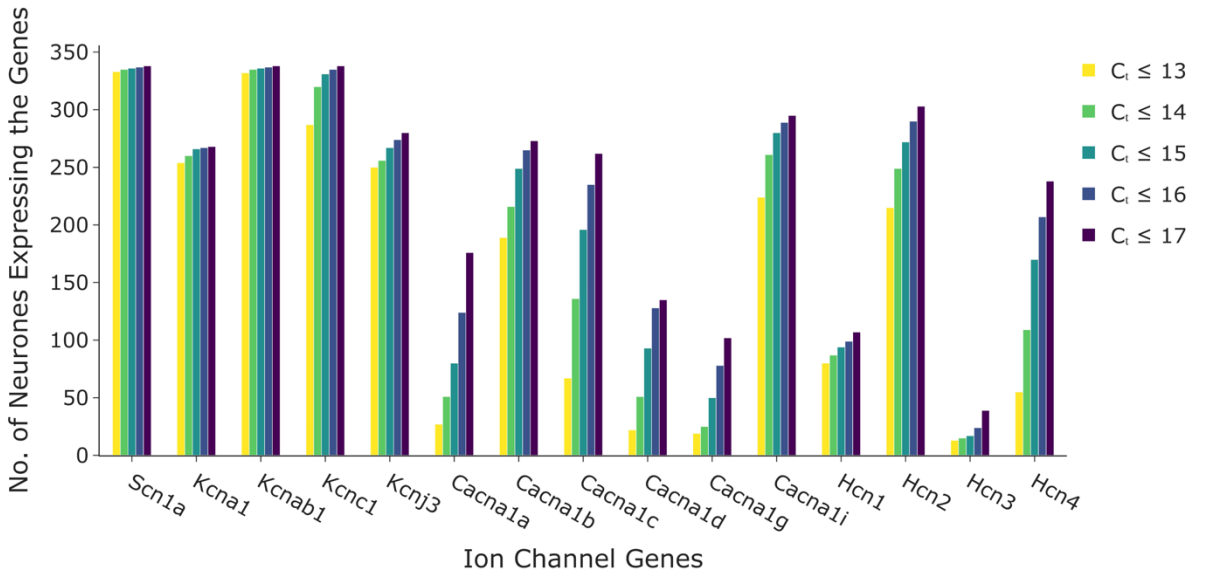

296

297 **Figure 2: Selection of expression threshold for filtering transcriptomics data.**
298 Number of neurons identified with each ion channel transcript at C_t values from 13–17.
299 $C_t \leq 15$ was chosen to denote ion channel presence.

300 Based on thresholding for the apparent presence or absence of the 15 ion channel
301 genes, coding for 14 different ion channels, from our thresholded transcriptomic
302 data, we identified 104 unique neuronal phenotypes from 321 sampled neurons
303 (Figure 3). A maximum of 13 of these ion channels were present in a neuronal
304 phenotype. Figure 3A shows these ordered from the most commonly (bottom) to
305 least commonly expressed ion channel gene. Three of the Ca^{2+} channel types
306 (*Cacna1g*, *Cacna1a*, *Cacna1d*) and two of the HCN types (1,3) were rarely present.
307 The frequency of each neuronal phenotype was non-uniform (Figure 3B). Fifty-
308 seven neuronal phenotypes occurred only once; the most common neuronal
309 phenotype occurred 22 times. 43% (137/321) of neurons belonged to 8 common
310 types with 14 or more cells in each neuronal phenotype: T4, T7, T14, T15, T23, T30,
311 T73, T91. While only 79/312 neurons expressed *HCN1*, the commonly occurring
312 types typically had the *HCN1* channel. Trends in *HCN2*, *HCN3*, and *HCN4* were not
313 associated with large increases in the number of occurrences of a neuronal
314 phenotype. We also examined sex-based differences in types and whether they
315 projected to the sinoatrial node (SAN). Three of the eight common types were from
316 the female, and T30 was found only in female, non-SAN-projecting neurons. There
317 were no statistically significant sex-dependent differences in ion channel expression
318 between the SAN-projecting and non-SAN-projecting RAGP neurons (Moss et al.,

2021).

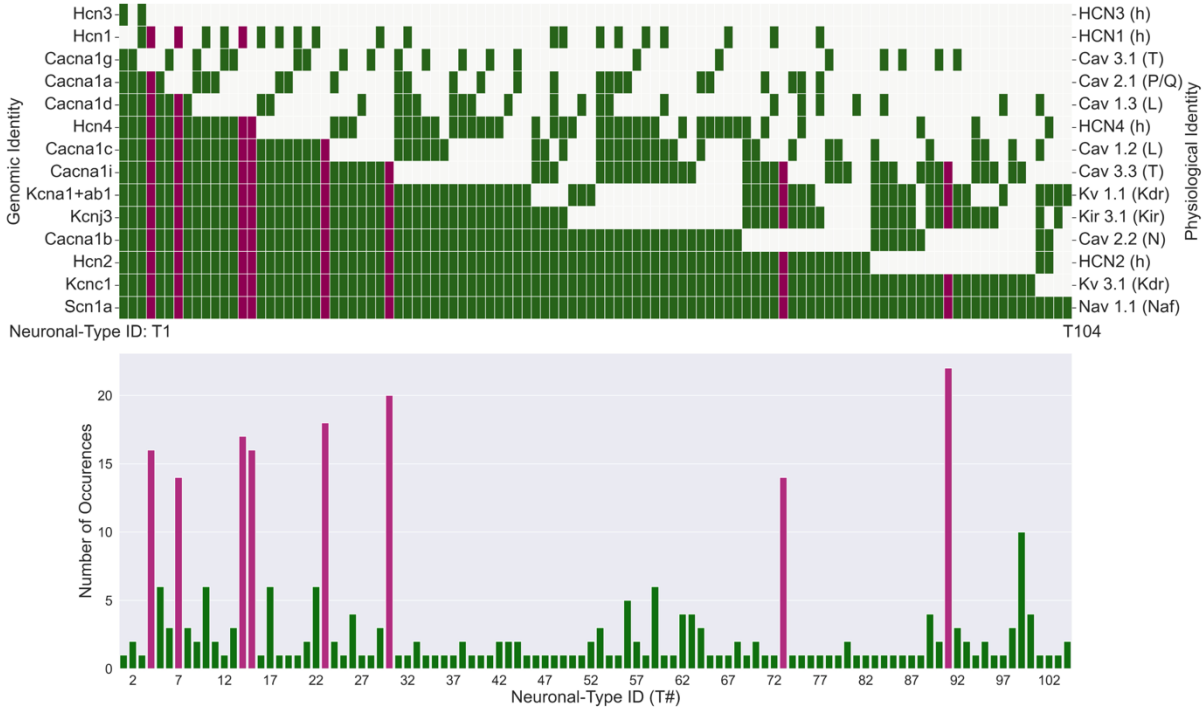

Figure 3: Neuronal phenotypes resulting from thresholded single neuron gene expression data on ion channels. Top: Binary map for the 104 unique channel combinations ordered by frequency of occurrence of ion channels. **Bottom:** Number of cells of each neuronal phenotype (321 cells, 104 types). The eight common neuronal phenotypes are highlighted in magenta, while the remaining neuronal phenotypes are in green.

Responses to current clamp for all neuronal phenotypes matched experimentally observed patterns found in multiple species (rodents, minipigs, dogs): phasic responses and tonic firing (Figure 4) (J. Andrew Armour, 1991; Edwards et al., 1995; Hanna et al., 2021; Harper & Adams, 2021; McAllen et al., 2011). As in experiments, electrophysiological responses were dependent on current clamp stimulus strength, such that some neurons would transition with increased input current (Figure 4A): 61% were phasic only (Figure 4B), 24% tonic only (Figure 4C), 11% phasic-to-tonic (Figure 4D), 3% were tonic-to-phasic (Figure 4E). The remaining firing patterns included stray occurrences of the artificial firing patterns (spontaneous firing, incomplete repolarization), which were filtered out and removed from our analysis. The primarily phasic and tonic firing patterns emerge from diverse combinations of ion channels that contribute to different dynamics in neuronal behaviors.

We used currentscapes (Alonso & Marder, 2019) to visualize the relative contribution of each ion channel to RMP, inward currents, and outward currents over time in a representative phasic (Figure S5 A) and tonic (Figure S5 B) neuron. We observed *Scn1a*, *Cacna1g* and *Cacna1i* to contribute substantially to the active phases of the action potential, while *Cacna1c* modulated the trough of repolarization. While *HCN3, 4* and *Kcnj3* dominated the RMP, *Kcnc1* and inactivating *Kcna1* influenced the repolarization phase of the spike. In the phasically firing neuron, *Kcnj3* has a much larger effect on outward currents than in the tonically firing neuron, which had outward currents dominated by *Kcnc1*.

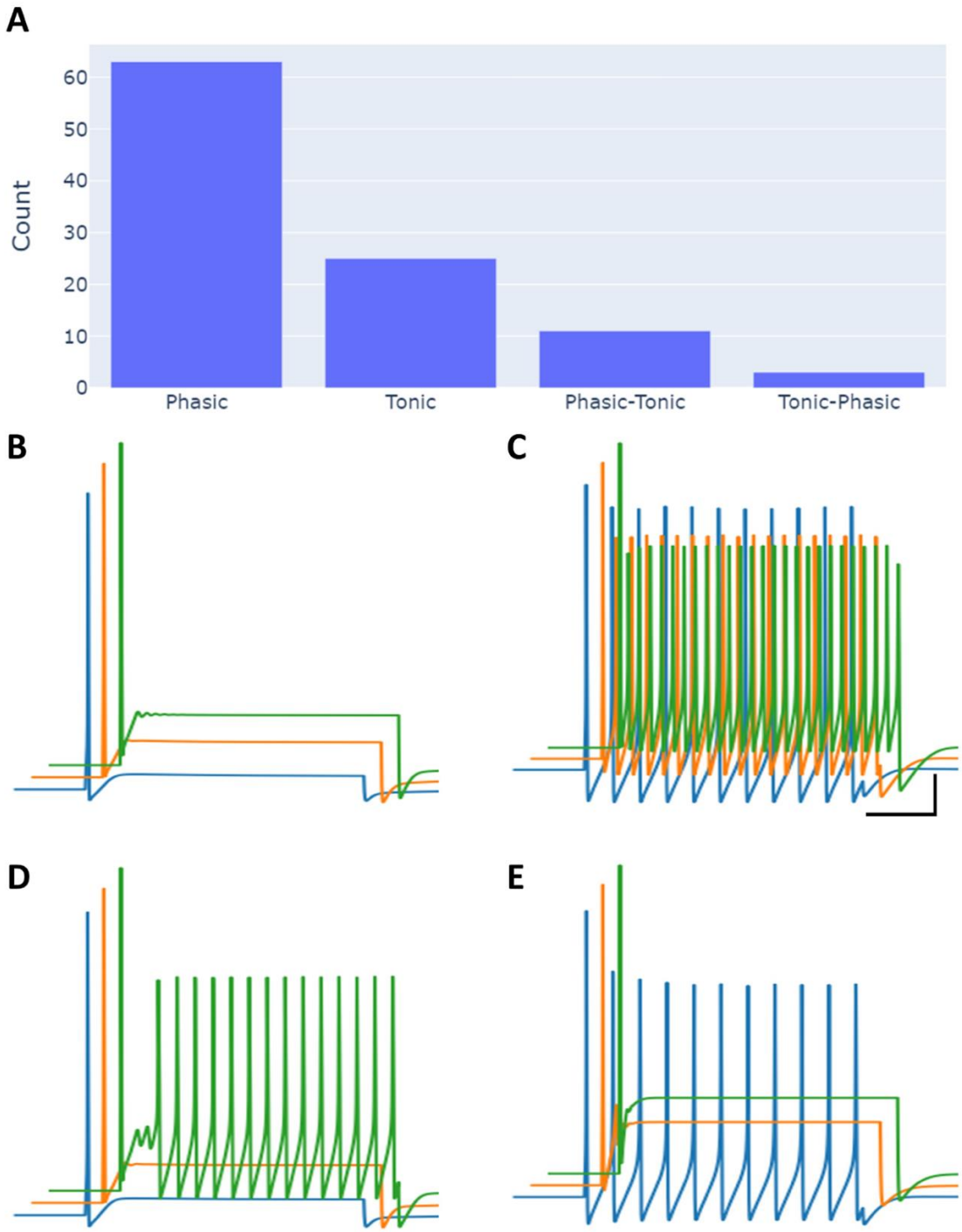

Figure 4: Neuronal firing behavior with increasing stimulus strength. (A) Number of neurons with each firing behavior. Example traces for **(B)** phasic (T1), **(C)** tonic (T51), **(D)** phasic-to-tonic (T2) **(E)** tonic-to-phasic (T52). Scale: 10 mV;100 ms. blue,orange,green: 0.1,0.3,0.5 nA stimulus.

The contributions of *Kcnc1* to tonic behavior were supported by a sensitivity analysis performed for a fixed current stimulus. Firing frequency was observed to be most

sensitive to *Kcnc1* and *Cacna1g*. AP peak was most sensitive to *Cacna1a* and inactivating *Kcna1*, while *Cacna1c* and *Kcnj3* affected the maximum hyperpolarization. Full width at half maximum was most regulated by *Cacna1b*. Each metric was most significantly affected by a different ion channel, highlighting the strength of using the single-cell transcriptomics to identify the combinations of ion channels present *in vivo*.

Current-frequency curves for tonically active neuronal models demonstrated a monotonic increase in frequency with increased current for all tonically-firing neurons (Figure 5). The slopes of the f–I curves were clustered into two groups. The neuronal phenotypes which expressed either both *Cacna1d*} and *Kcna1+ab1* (inactivating *Kcna1*) or neither, had slopes greater than the best-fit line. The neuronal phenotypes which expressed *Cacna1d* but lacked *Kcna1+ab1* had slopes less than the best-fit line. Despite these differences, the firing frequencies of our neuronal models ranged between 12 – 65 Hz for a stimulus range of 0.01 – 0.5 nA, which is within the experimentally observed limits of 5 – 60 Hz (guinea-pigs: 5 Hz, rats: 9 – 15 Hz, mice: 2 – 60 Hz, dogs: 60 Hz, and humans between 20 – 50 Hz) (Edwards et al., 1995; McAllen et al., 2011; Tompkins et al., 2024).

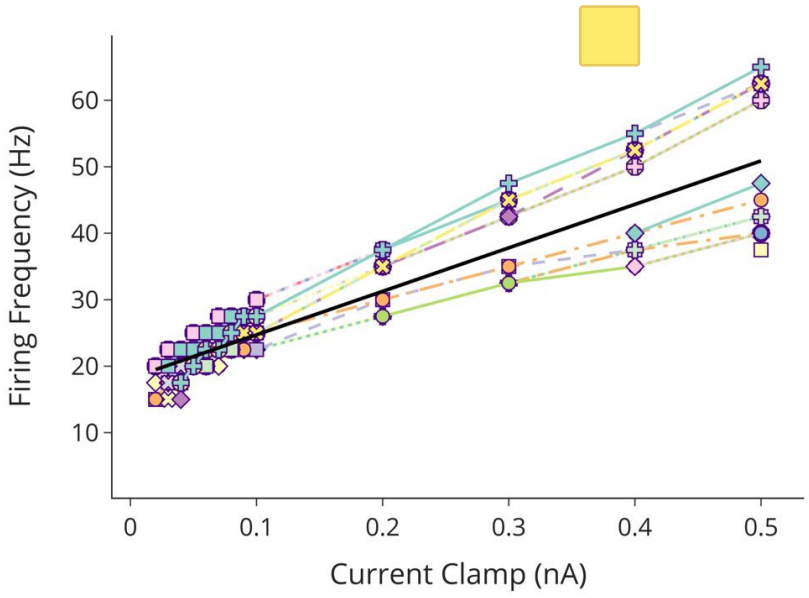

Figure 5: Current-frequency relationship for tonically firing neurons. Data fit (black line) with slope 60.5 Hz/nA. Each color represents a different neuronal phenotype.

Discussion

Computational systems biology approach augments electrophysiology data

Biophysical models have long been limited by the electrophysiology data available, sparse in most species due to the time and skill required to collect it, and almost entirely unavailable for humans. Sample sizes for electrophysiology datasets are also limited, while transcriptomic data can be gathered more quickly and obtained in quantities of hundreds to thousands of single-cells (Moss et al., 2021; Zhao et al., 2022). Therefore, transcriptomics coupled with a computational systems biology approach can be used as a complementary resource that will allow more rapid development of extensive cell activity libraries (McDougal et al., 2017; Podlaski et al., 2017).

We aimed to connect single-neuron transcriptomics data to cellular electrophysiology with quantitatively validated electrophysiological models. Our model is the latest iteration of our work to understand ion channel contributions to electrophysiological behavior and cardiovascular regulation (Schwaber et al., 1993; Vadigepalli et al., 2001), made possible by the increasing availability of single-cell transcriptomics data. Despite limitations due to gaps in datasets containing both transcriptomic data and electrophysiological recordings in ICNS neurons as are available for other neuronal classes in the brain (Bernaerts et al., 2023; Nandi et al., 2022), we developed a library of biophysically-constrained ICNS parallel conductance models. In this paper, we propose an alternative modelling approach, built on the basis of the more widely available and fine-grained transcriptomics data to create electrophysiological models that match the distribution of behavior observed in populations of similar neurons (Edwards et al., 1995; McAllen et al., 2011; Tompkins et al., 2024). The advantage of our approach is that the low throughput and laborious process of collecting electrophysiology data can be augmented by combining it with computational approaches to effectively increase the sample size.

Distribution of tonic and phasic firing patterns

Our model yielded 61% phasic, 24% tonic, 11% phasic-to-tonic, 3% tonic-to-phasic and ~1% artificial firing patterns (spontaneous firing, incomplete repolarization). Our

model parameters were additionally tuned to ensure that the model does not generate firing patterns that are artifacts of the modelling paradigm (*see* **Materials and Methods**). Despite generating physiologically observable patterns, the presence of these trace firing patterns lead us to hypothesize that either the transcriptomic sequences of ion channels in those respective neuronal phenotypes are inadequately identified, or these neuronal types may have been erroneously identified as a RAGP PN, whereas it may be a non-excitable neuron. Thus, the strength of our workflow can be additionally employed to enhance experimental protocols and insights.

The dominant firing behavior in our models was phasic over a range of 0.1 – 0.5 nA current clamp stimulus. Minipig, dog, and rat ICNS neurons show dominantly phasic responses to current clamp (McAllen et al., 2011; Tompkins et al., 2024; Xi et al., 1994), consistent with our model, which was based on Yucatán minipig transcriptomic data. Different studies on guinea pig neurons have reported them to be either phasic (Hoover et al., 2009), or tonic (Edwards et al., 1995). By contrast, human neurons show predominantly tonic responses (Edwards et al., 1995; Tompkins et al., 2024). It will be interesting to see if transcriptomic differences across species can be used to predict these electrophysiological differences.

Strengths and limitations of the model

A significant challenge for our approach remains the unknown effects of several steps between mRNA transcription and placement of ion channels in the membrane: post-transcription processing, translation and post-translational processing, subunit aggregation, and differential channel placement in dendrites, soma, and axons. Owing to these factors, the direct use of cycle threshold as an indicator of ion channel density was not successful. Instead, we employed a novel cutoff technique to binarize transcriptomic data into ion channel presence or absence in a neuron if the cycle threshold was above or below a fifteen. Proteomic data would be closer to the physiological product and, therefore, should be more useful in improving omic-to-model translation by providing a one-to-one match between the genetic and electrophysiological profiles. Alternatively, patch-clamp data, alongside transcriptomic data and electrophysiology data from the same cell could further enhance model translation (Bernaerts et al., 2023). Patch-clamp has been used to

generate models which demonstrated predicted conductances to reflect gene expression differences (Nandi et al., 2022). However, patch-clamp data use is still limited by its low throughput.

A further limitation in the use of transcriptomics data arose because of limitations in the ion channel models found in databases. These were derived either from large cells such as mammalian cortical pyramidal cells or from gene expression in oocytes, human embryonic kidney (HEK) cells, or other heterologous cell types (McDougal et al., 2017; Podlaski et al., 2017; Ranjan et al., 2011), any of which will have dynamics different than that of similar channels from RAGP neurons. In particular, we encountered this difficulty with the Na^+ channel, a channel that is particularly difficult to measure in voltage clamp due to fast kinetics. Multiple isomers of this channel distributed along dendrites and axons of different neurons, possess different kinetics. To assess the sensitivity of the kinetic parameters of the Na^+ channel we varied the inactivation parameter (h_∞) by ±20% (Figure S6). Increases in the slope shifted the distribution of electrophysiological behavior so that phasic-tonic and tonic behaviors were predominant. Decreases in the slope maintained the predominance of phasic behavior. Of the alternative Na^+ channel models considered, two models had similar h_∞ values while one model had an inactivation parameter two times higher (Table S1). Thus, the uncertainty of kinetic parameters in ion channel models should be considered when analyzing the model predictions. Both electrophysiological recordings and modelling of single isolated neurons are also limited by the artificiality of current-clamp inputs. The use of spike train inputs based on vagal recordings and cellular recordings from intact ganglion preparations will allow further development and refinement of computational models (Machhada et al., 2015; Rentero et al., 2002).

Several planned extensions of the current model will address some of these limitations. The most immediate extension is to link the single-neuron models into a ICNS network model. One way to do this would be to add synapse models based on electrophysiology data (McAllen et al., 2011) and connect the neurons based on neural tracing data (Cheng et al., 2004). The implementation of spike train stimuli from vagal recordings could then be used as inputs to the model to test it against ICNS electrophysiology (Machhada et al., 2015; Rentero et al., 2002).

Our model is also primed to be coupled with other cardiovascular physiology models to address questions on ICNS regulation of heart function (Gee, Lenhoff, et al., 2023; Park et al., 2020). In the context of ICNS function in cardiovascular regulation, we hypothesize that the neurons predisposed towards phasic and tonic behavior may have different functions. Due to their higher firing rate, the tonic neural activity may carry beat-to-beat tone from the nucleus ambiguus (NA) via the vagus to regulate heart rate, while phasically firing neurons may regulate contractility with slower drive from the dorsal motor nucleus of the vagus (DMV). This is supported in part by neural tracing studies, which showed the NA and DMV project to distinct populations of principal neurons within the same ICNS ganglion, extending the two separate lanes of vagal tone from the brainstem to the ICNS (Cheng et al., 2004; Gee, Hornung, et al., 2023). Physiological evidence also supports the notion of two distinct vagal lanes, as different ICNS neuronal clusters, such as the RAGP, have been found to primarily regulate heart rate versus contractility (Fedele & Brand, 2020; Gourine et al., 2016). Our model, in the present state, could be incorporated as a module in a larger systemic models of autonomic regulation and cardiovascular function (Gee, Lenhoff, et al., 2023; Park et al., 2020) to test the functional implications of this hypothesized connectivity.

Conclusion

We demonstrate a novel workflow to bridge the gap between molecular-level gene expression and cellular-level electrophysiological function, using single-neuron HT-qPCR data from RAGP neurons to derive ion channel combinations that generate a library of single-neuron parallel conductance models (Figure 1). In order to develop biophysically detailed models from single-cell transcriptomics data, we use single-neuron HT-qPCR ion channel data from RAGP principal neurons to quantitatively derive ion channel combinations that generate a library of single-neuron parallel conductance models. We used a gene expression threshold to select the presence or absence of ion channels in each parallel conductance model. After thresholding, 104 unique ion channel combinations were identified from the 321 single-neuron transcriptomic samples (Figure 3). The emergent firing patterns were in agreement with experimental reports (Figure 4). By this approach, we demonstrate a use case of computational modelling to relate molecular data to the electrical behavior of

neurons. This library of transcriptomics-based single-neuron models provides a framework for developing parallel conductance models of neurons from other regions and provides a platform for developing network models that represent the interactions of various neuronal phenotypes involved in cardiovascular regulation.

References

Allen, N. M., Weckhuysen, S., Gorman, K., King, M. D., & Lerche, H. (2020). Genetic potassium channel-associated epilepsies: Clinical review of the Kv family. *European Journal of Paediatric Neurology: EJPN: Official Journal of the European Paediatric Neurology Society*, *24*, 105–116.

Alonso, L. M., & Marder, E. (2019). Visualization of currents in neural models with similar behavior and different conductance densities. *ELife*, *8*. https://doi.org/10.7554/eLife.42722

Armour, J. A. (2008). Potential clinical relevance of the “little brain” on the mammalian heart. *Experimental Physiology*, *93*(2), 165–176.

Armour, J. Andrew. (1991). Intrinsic Cardiac Neurons. *Journal of Cardiovascular Electrophysiology*, *2*(4), 331–341.

Beaumont, E., Wright, G. L., Southerland, E. M., Li, Y., Chui, R., KenKnight, B. H., Armour, J. A., & Ardell, J. L. (2016). Vagus nerve stimulation mitigates intrinsic cardiac neuronal remodelling and cardiac hypertrophy induced by chronic pressure overload in guinea pig. *American Journal of Physiology. Heart and Circulatory Physiology*, *310*(10), H1349-59.

Bernaerts, Y., Deistler, M., Gonçalves, P. J., Beck, J., Stimberg, M., Scala, F., Tolias, A. S., Macke, J., Kobak, D., & Berens, P. (2023). Combined statistical-mechanistic modelling links ion channel genes to physiology of cortical neuron types. In *bioRxiv* (p. 2023.03.02.530774). https://doi.org/10.1101/2023.03.02.530774

Carnevale, N. T., & Hines, M. L. (2006). *The NEURON Book*. Cambridge University Press.

Cheng, Z., Zhang, H., Guo, S. Z., Wurster, R., & Gozal, D. (2004). Differential control over postganglionic neurons in rat cardiac ganglia by NA and DmnX neurons: anatomical evidence. *American Journal of Physiology. Regulatory, Integrative and Comparative Physiology*, *286*(4), R625-33.

Drion, G., O’Leary, T., & Marder, E. (2015). Ion channel degeneracy enables robust and tunable neuronal firing rates. *Proceedings of the National Academy of Sciences of the United States of America*, *112*(38), E5361-70.

Dura-Bernal, S., Suter, B. A., Gleeson, P., Cantarelli, M., Quintana, A., Rodriguez, F., Kedziora, D. J., Chadderdon, G. L., Kerr, C. C., Neymotin, S. A., McDougal, R. A., Hines, M., Shepherd, G. M., & Lytton, W. W. (2019). NetPyNE, a tool for data-

542 driven multiscale modelling of brain circuits. *ELife*, *8*.
543 https://doi.org/10.7554/eLife.44494
544 Edwards, F. R., Hirst, G. D., Klemm, M. F., & Steele, P. A. (1995). Different types of
545 ganglion cell in the cardiac plexus of guinea-pigs. *The Journal of Physiology*, *486 (*
546 *Pt 2)*, 453–471.
547 Erdemir, A., Mulugeta, L., Ku, J. P., Drach, A., Horner, M., Morrison, T. M., Peng, G.
548 C. Y., Vadigepalli, R., Lytton, W. W., & Myers, J. G., Jr. (2020). Credible practice of
549 modelling and simulation in healthcare: ten rules from a multidisciplinary
550 perspective. *Journal of Translational Medicine*, *18*(1), 369.
551 Fedele, L., & Brand, T. (2020). The Intrinsic Cardiac Nervous System and Its Role in
552 Cardiac Pacemaking and Conduction. *Journal of Cardiovascular Development and*
553 *Disease*, *7*(4). https://doi.org/10.3390/jcdd7040054
554 Gee, M. M., Hornung, E., Gupta, S., Newton, A. J. H., Cheng, Z. J., Lytton, W. W.,
555 Lenhoff, A. M., Schwaber, J. S., & Vadigepalli, R. (2023). Unpacking the
556 multimodal, multi-scale data of the fast and slow lanes of the cardiac vagus through
557 computational modelling. *Experimental Physiology*.
558 https://doi.org/10.1113/EP090865
559 Gee, M. M., Lenhoff, A. M., Schwaber, J. S., Ogunnaike, B. A., & Vadigepalli, R.
560 (2023). Closed-loop modelling of central and intrinsic cardiac nervous system
561 circuits underlying cardiovascular control. *AIChE Journal. American Institute of*
562 *Chemical Engineers*, *69*(4). https://doi.org/10.1002/aic.18033
563 Goaillard, J.-M., & Marder, E. (2021). Ion Channel Degeneracy, Variability, and
564 Covariation in Neuron and Circuit Resilience. *Annual Review of Neuroscience*, *44*,
565 335–357.
566 Gourine, A. V., Machhada, A., Trapp, S., & Spyer, K. M. (2016). Cardiac vagal
567 preganglionic neurones: An update. *Autonomic Neuroscience: Basic & Clinical*,
568 *199*, 24–28.
569 Hadaya, J., & Ardell, J. L. (2020). Autonomic Modulation for Cardiovascular Disease.
570 *Frontiers in Physiology*, *11*, 617459.
571 Hanna, P., Dacey, M. J., Brennan, J., Moss, A., Robbins, S., Achanta, S., Biscola, N.
572 P., Swid, M. A., Rajendran, P. S., Mori, S., Hadaya, J. E., Smith, E. H., Peirce, S.
573 G., Chen, J., Havton, L. A., Cheng, Z. J., Vadigepalli, R., Schwaber, J., Lux, R. L.,
574 … Shivkumar, K. (2021). Innervation and Neuronal Control of the Mammalian
575 Sinoatrial Node a Comprehensive Atlas. *Circulation Research*, *128*(9), 1279–1296.

576 Harper, A. A., & Adams, D. J. (2021). Electrical properties and synaptic transmission
577 in mouse intracardiac ganglion neurons in situ. *Physiological Reports*, *9*(18),
578 e15056.
579 Heinemann, S. H., Rettig, J., Graack, H. R., & Pongs, O. (1996). Functional
580 characterization of Kv channel beta-subunits from rat brain. *The Journal of*
581 *Physiology*, *493*(3), 625–633.
582 Hille, B. (n.d.). *Ionic Channels of Excitable Membranes (1992)* (2nd ed.).
583 Hoover, D. B., Tompkins, J. D., & Parsons, R. L. (2009). Differential activation of
584 guinea pig intrinsic cardiac neurons by the PAC1 agonists maxadilan and pituitary
585 adenylate cyclase-activating polypeptide 27 (PACAP27). *The Journal of*
586 *Pharmacology and Experimental Therapeutics*, *331*(1), 197–203.
587 Lizot, G., Pasqualin, C., Tissot, A., Pagès, S., Faivre, J.-F., & Chatelier, A. (2022).
588 Molecular and functional characterization of the mouse intrinsic cardiac nervous
589 system. *Heart Rhythm: The Official Journal of the Heart Rhythm Society*, *19*(8),
590 1352–1362.
591 Machhada, A., Ang, R., Ackland, G. L., Ninkina, N., Buchman, V. L., Lythgoe, M. F.,
592 Trapp, S., Tinker, A., Marina, N., & Gourine, A. V. (2015). Control of ventricular
593 excitability by neurons of the dorsal motor nucleus of the vagus nerve. *Heart*
594 *Rhythm: The Official Journal of the Heart Rhythm Society*, *12*(11), 2285–2293.
595 McAllen, R. M., Salo, L. M., Paton, J. F. R., & Pickering, A. E. (2011). Processing of
596 central and reflex vagal drives by rat cardiac ganglion neurones: an intracellular
597 analysis. *The Journal of Physiology*, *589*(Pt 23), 5801–5818.
598 McDougal, R. A., Morse, T. M., Carnevale, T., Marenco, L., Wang, R., Migliore, M.,
599 Miller, P. L., Shepherd, G. M., & Hines, M. L. (2017). Twenty years of ModelDB and
600 beyond: building essential modelling tools for the future of neuroscience. *Journal of*
601 *Computational Neuroscience*, *42*(1), 1–10.
602 Moss, A., Robbins, S., Achanta, S., Kuttippurathu, L., Turick, S., Nieves, S., Hanna,
603 P., Smith, E. H., Hoover, D. B., Chen, J., Cheng, Z. J., Ardell, J. L., Shivkumar, K.,
604 Schwaber, J. S., & Vadigepalli, R. (2021). A single cell transcriptomics map of
605 paracrine networks in the intrinsic cardiac nervous system. *IScience*, *24*(7),
606 102713.
607 Mulugeta, L., Drach, A., Erdemir, A., Hunt, C. A., Horner, M., Ku, J. P., Myers, J. G.,
608 Jr, Vadigepalli, R., & Lytton, W. W. (2018). Credibility, Replicability, and
609 Reproducibility in Simulation for Biomedicine and Clinical Applications in

Neuroscience. In *Frontiers in Neuroinformatics* (Vol. 12). https://doi.org/10.3389/fninf.2018.00018

Nandi, A., Chartrand, T., Van Geit, W., Buchin, A., Yao, Z., Lee, S. Y., Wei, Y., Kalmbach, B., Lee, B., Lein, E., Berg, J., Sümbül, U., Koch, C., Tasic, B., & Anastassiou, C. A. (2022). Single-neuron models linking electrophysiology, morphology, and transcriptomics across cortical cell types. *Cell Reports*, *41*(6), 111659.

Park, J. H., Gorky, J., Ogunnaike, B., Vadigepalli, R., & Schwaber, J. S. (2020). Investigating the Effects of Brainstem Neuronal Adaptation on Cardiovascular Homeostasis. *Frontiers in Neuroscience*, *14*, 470.

Podlaski, W. F., Seeholzer, A., Groschner, L. N., Miesenböck, G., Ranjan, R., & Vogels, T. P. (2017). Mapping the function of neuronal ion channels in model and experiment. *ELife*, *6*. https://doi.org/10.7554/eLife.22152

Ranjan, R., Khazen, G., Gambazzi, L., Ramaswamy, S., Hill, S. L., Schürmann, F., & Markram, H. (2011). Channelpedia: an integrative and interactive database for ion channels. *Frontiers in Neuroinformatics*, *5*, 36.

Rentero, N., Cividjian, A., Trevaks, D., Pequignot, J. M., Quintin, L., & McAllen, R. M. (2002). Activity patterns of cardiac vagal motoneurons in rat nucleus ambiguus. *American Journal of Physiology. Regulatory, Integrative and Comparative Physiology*, *283*(6), R1327-34.

Rettig, J., Heinemann, S. H., Wunder, F., Lorra, C., Parcej, D. N., Dolly, J. O., & Pongs, O. (1994). Inactivation properties of voltage-gated K+ channels altered by presence of beta-subunit. *Nature*, *369*(6478), 289–294.

Rothman, J. S., & Manis, P. B. (2003a). Differential expression of three distinct potassium currents in the ventral cochlear nucleus. *Journal of Neurophysiology*, *89*(6), 3070–3082.

Rothman, J. S., & Manis, P. B. (2003b). Kinetic analyses of three distinct potassium conductances in ventral cochlear nucleus neurons. *Journal of Neurophysiology*, *89*(6), 3083–3096.

Rothman, J. S., & Manis, P. B. (2003c). The roles potassium currents play in regulating the electrical activity of ventral cochlear nucleus neurons. *Journal of Neurophysiology*, *89*(6), 3097–3113.

642 Roy, R., & Narayanan, R. (2023). Ion-channel degeneracy and heterogeneities in the
643 emergence of complex spike bursts in CA3 pyramidal neurons. *The Journal of*
644 *Physiology*, *601*(15), 3297–3328.
645 Rybak, I. A., Paton, J. F., & Schwaber, J. S. (1997). Modelling neural mechanisms for
646 genesis of respiratory rhythm and pattern. I. Models of respiratory neurons. *Journal*
647 *of Neurophysiology*, *77*(4), 1994–2006.
648 Salavatian, S., Beaumont, E., Longpré, J.-P., Armour, J. A., Vinet, A., Jacquemet, V.,
649 Shivkumar, K., & Ardell, J. L. (2016). Vagal stimulation targets select populations of
650 intrinsic cardiac neurons to control neurally induced atrial fibrillation. *American*
651 *Journal of Physiology. Heart and Circulatory Physiology*, *311*(5), H1311–H1320.
652 Schwaber, J. S., Graves, E. B., & Paton, J. F. (1993). Computational modelling of
653 neuronal dynamics for systems analysis: application to neurons of the
654 cardiorespiratory NTS in the rat. *Brain Research*, *604*(1–2), 126–141.
655 Selyanko, A. A. (1992). Membrane properties and firing characteristics of rat cardiac
656 neurones in vitro. *Journal of the Autonomic Nervous System*, *39*(3), 181–189.
657 Sewing, S., Roeper, J., & Pongs, O. (1996). Kvβ1 Subunit Binding Specific for
658 Shaker-Related Potassium Channel α Subunits. *Neuron*, *16*(2), 455–463.
659 Shevtsova, N. A., Ha, N. T., Rybak, I. A., & Dougherty, K. J. (2020). Neural
660 Interactions in Developing Rhythmogenic Spinal Networks: Insights From
661 Computational Modelling. *Frontiers in Neural Circuits*, *14*, 614615.
662 Song, W. J. (2002). Genes responsible for native depolarization-activated K+
663 currents in neurons. *Neuroscience Research*, *42*(1), 7–14.
664 Tompkins, J. D., Hoover, D. B., Havton, L. A., Patel, J. C., Cho, Y., Smith, E. H.,
665 Biscola, N. P., Ajijola, O. A., Shivkumar, K., & Ardell, J. L. (2024). Comparative
666 specialization of intrinsic cardiac neurons in humans, mice, and pigs. *BioRxiv : The*
667 *Preprint Server for Biology*. https://doi.org/10.1101/2024.04.04.588174
668 Vadigepalli, R., Doyle, F. J., & Schwaber, J. S. (2001). Analysis and neuronal
669 modelling of the nonlinear characteristics of a local cardiac reflex in the rat. *Neural*
670 *Computation*, *13*(10), 2239–2271.
671 Vaseghi, M., Salavatian, S., Rajendran, P. S., Yagishita, D., Woodward, W. R.,
672 Hamon, D., Yamakawa, K., Irie, T., Habecker, B. A., & Shivkumar, K. (2017).
673 Parasympathetic dysfunction and antiarrhythmic effect of vagal nerve stimulation
674 following myocardial infarction. *JCI Insight*, *2*(16).
675 https://doi.org/10.1172/jci.insight.86715

Xi, X., Randall, W. C., & Wurster, R. D. (1994). Electrophysiological properties of canine cardiac ganglion cell types. *Journal of the Autonomic Nervous System*, *47*(1–2), 69–74.

Zhao, Q., Yu, C. D., Wang, R., Xu, Q. J., Dai Pra, R., Zhang, L., & Chang, R. B. (2022). A multidimensional coding architecture of the vagal interoceptive system. *Nature*, *603*(7903), 878–884.

Additional information

Data Availability Statement

The model source and analysis code is available on Github (https://github.com/Daniel-Baugh-Institute/BiophysicalModellingOfIntrinsicCardiacNeurons) and the SPARC portal (https://sparc.science/). Model source code is also available through ModelDB (https://modeldb.science/2014824). The model can also be accessed through the simulation platform oSPARC (https://osparc.io/), which enables users to run simulations with the model using a Graphical User Interface.

Conflict of Interest Statement

The authors declare that the research was conducted in the absence of any commercial or financial relationships that could be construed as a potential conflict of interest.

Author Contributions

W.W.L., R.V., J.S.S, conceived, supervised the work and provided significant editorial contributions. S.G. worked on model development, validation, analysis, interpretation and visualisation of data. A.J.H.N and W.W.L. handled NetPyNE software development, designing and implementation of the sobol algorithm. S.G. and L.K. worked on building the model and ion channel library. A.M. and L.K assisted in the interpretation of transcriptomics data. S.G. and M.M.G. wrote the manuscript with edits from J.D.T., J.S.S., R.V. and W.W.L. All authors provided critical feedback to improve the manuscript.

Funding

National Heart, Lung, and Blood Institute (NHLBI) U01 HL133360 and R01 HL161696: J.S., R.V.; National Institutes of Health (NIH) Common Fund Stimulating

Peripheral Activity to Relieve Conditions (SPARC) Program OT2OD030534: R.V.; National Science Foundation (NSF) 1940700: M.G.

Acknowledgments

We would like to express our gratitude to Professor Robin McAllen for his insights and inputs which aided our model development and validation. We would also like to thank Professor Babatunde A. Ogunnaike for his mentorship. We are grateful to Siyan Guo and Joy Wang for reproducing current clamp simulations for neuron T54 from an earlier draft of this manuscript, and to Dr. Sujata Patil for reproducing the figures from the analysis code as part of 10 rules for Credible Practice of Modelling and Simulation in Biomedicine.

Keywords

autonomic regulation, systems biology, ion channels, Hodgkin-Huxley model, vagus nerve, intrinsic cardiac nervous system

Supplemental Data

Supplemental Figures (S1 – S7)

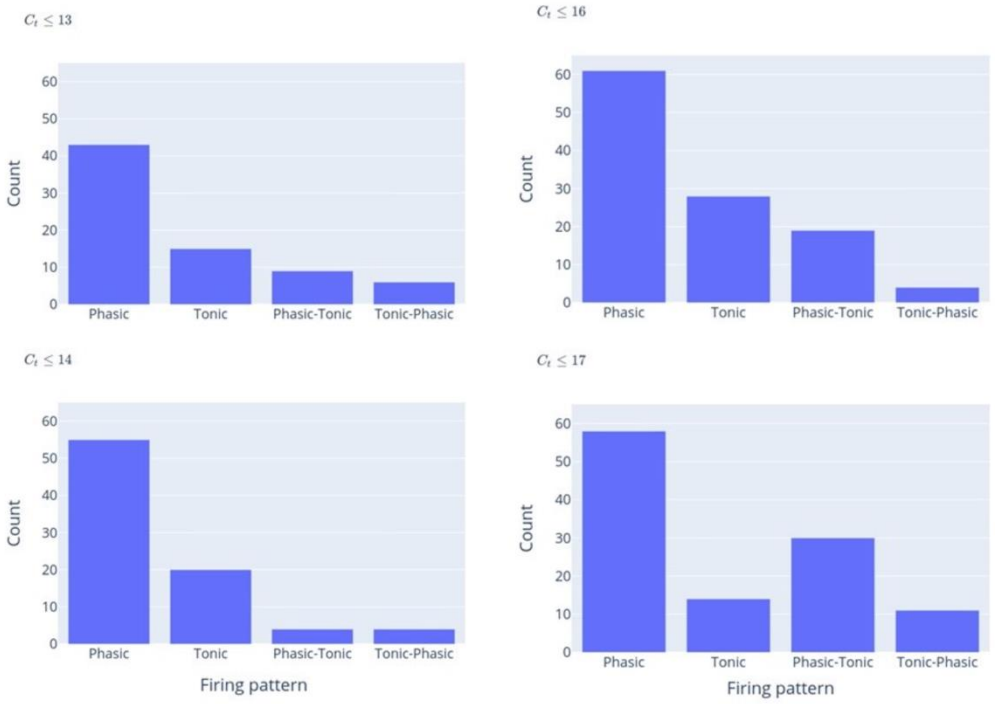

Figure S1: Distribution of firing behaviors for Ct thresholds varying from 13 – 17. The firing behavior of each neuronal phenotype was classified at step input stimulus intensities of 0.1, 0.3, and 0.5 nA. Despite the changing Ct threshold values, the dominant firing behavior remained phasic. For Ct threshold values ranging from 13 – 16, similar distributions for phasic, tonic, phasic-to-tonic, and tonic-to-phasic were observed. For Ct ≤ 17, phasic-to-tonic behavior became more common than tonic behavior.

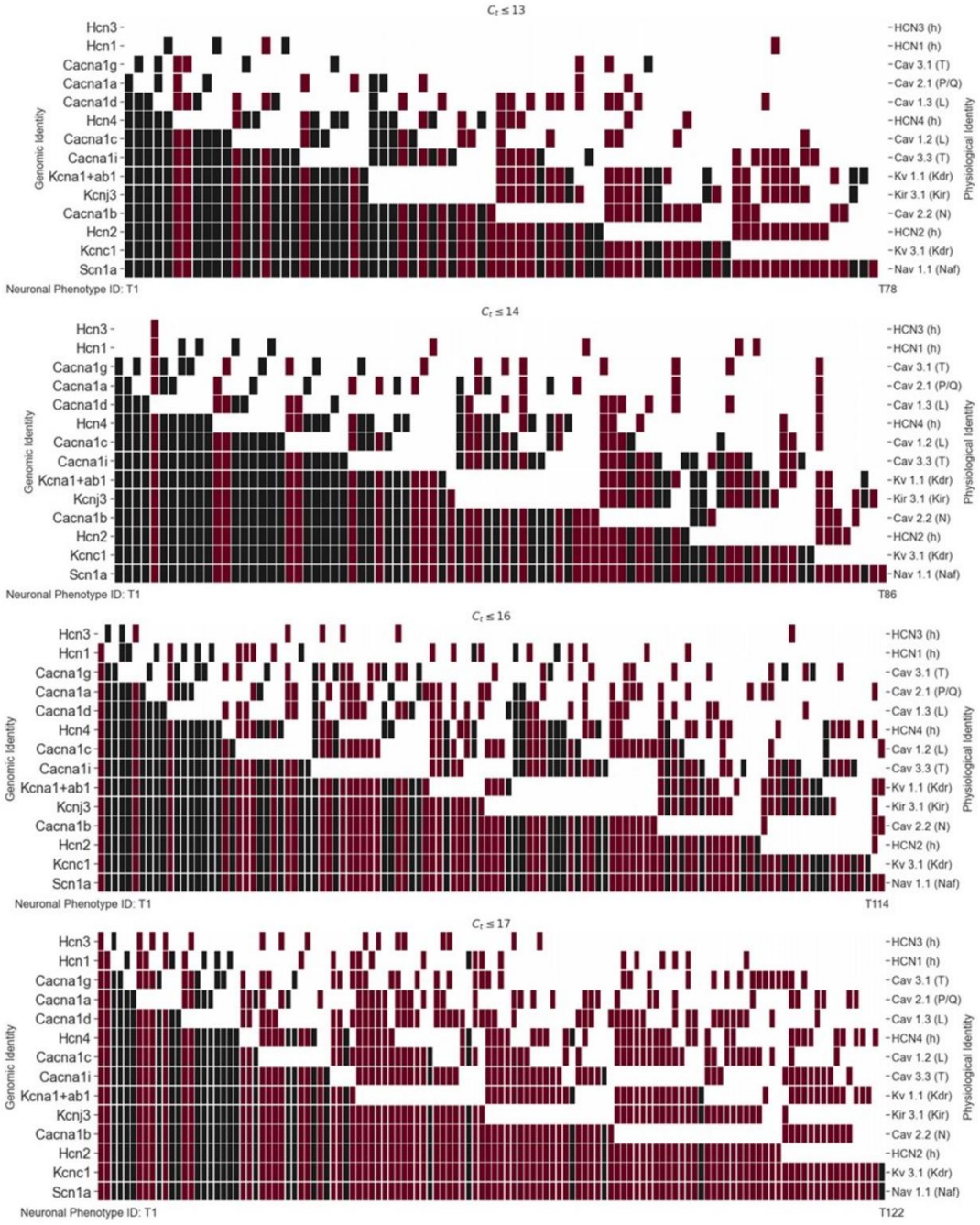

Figure S1: Variability in the transcriptomics map for different C_t values explored resulting in the emergence of newer neuronal phenotypes. Neuronal phenotypes based on C_t thresholds varying from 13 – 17. New neuronal types not defined by thresholding transcriptomic data with $C_t \leq 15$ are highlighted in red. Neuronal types are sorted using the same method as in Figure 3, based on the number of genes expressed and the frequency that a gene is expressed. The percent of new neuronal phenotypes for C_t values 13, 14, 16, and 17 is 53%, 47%, 56%, and 77%. While this is a high percentage of the neuronal phenotypes, further

761 analysis of the frequency of these new neuronal phenotypes revealed that they
762 account for only 11-20% of the cells

763

764 **Figure S2: Distribution of neuronal phenotype occurrences that were defined**
765 **with $C_t \leq 15$ with C_t threshold value varying from 13 – 17.** Neuronal phenotypes
766 with more than ten occurrences are highlighted in pink. When using a different C_t
767 threshold value, neuronal-types that did not fit into any neuronal-type found with $C_t \leq$
768 15 are not shown in the plot. New neuronal transcriptional phenotypes appear at
769 different C_t thresholds, but they only account for 11-20% of the cells. We also found
770 that all C_t thresholds still produced just 5-8 common neuronal phenotypes with 10 or
771 more occurrences containing 25-40% of the cells, suggesting that the frequency of
772 occurrences of the neuronal phenotypes remains relatively similar across C_t
773 threshold values.

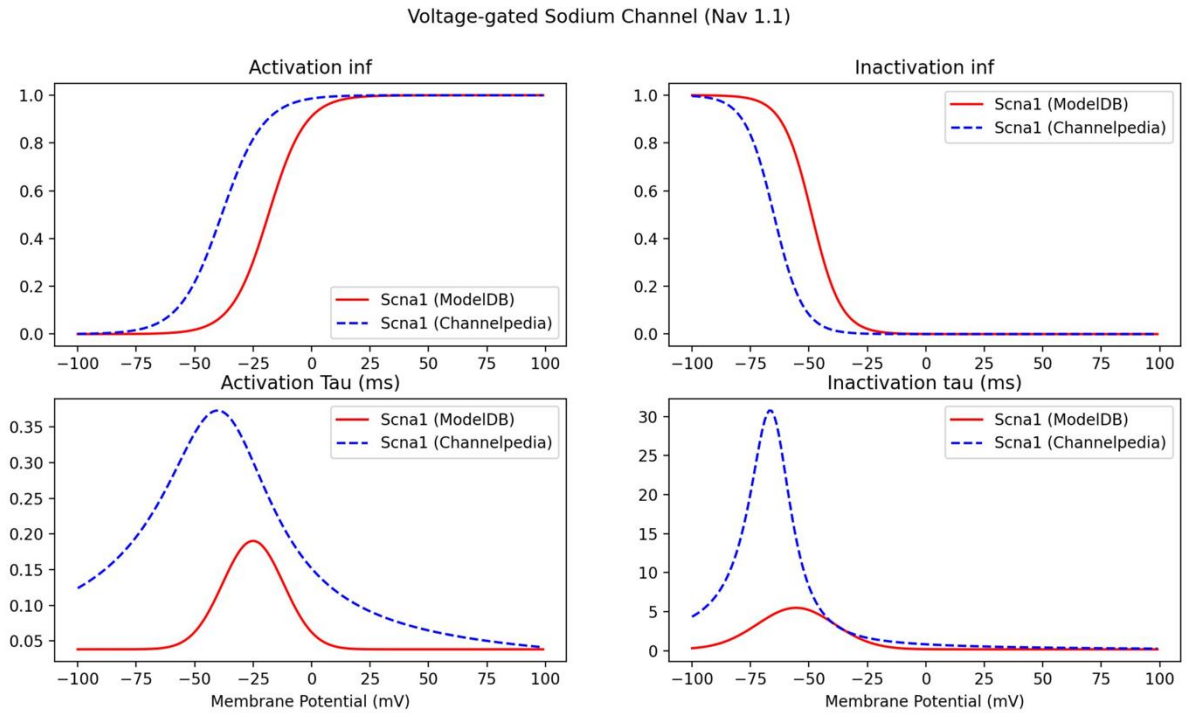

Figure S3: Comparison of Nav1.1 activation and inactivation curves for alternative ion channel models. The models compared are Channelpedia ID #35 and ModelDB Accession #264834. We identified five alternative Nav1.1 models, of which, 3 were unsuitable due to a large window current which required an unphysiologically large reversal potential to compensate for the current at rest, or a very leaky cell (large R_{in}). To choose between the remaining two models (Channelpedia ID #35 and ModelDB Accession #264834), we assessed the rheobase. Comparison of the two Na^+ channel candidates in the full parallel conductance model identified Channelpedia ID #35 as a better fit.

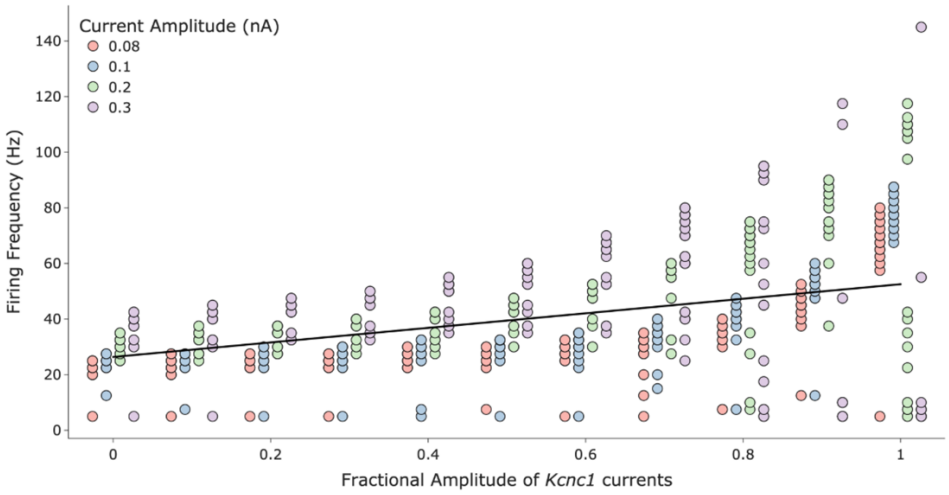

787

788 **Figure S4: Variation of the firing frequency with respect to the ϕ_{Kcnc1} for**
789 **different current clamp stimuli surveyed.** An optimized best-fit (black line) indicate
790 an increase of 2.62 Hz per 0.1 increase in fractional amplitude.

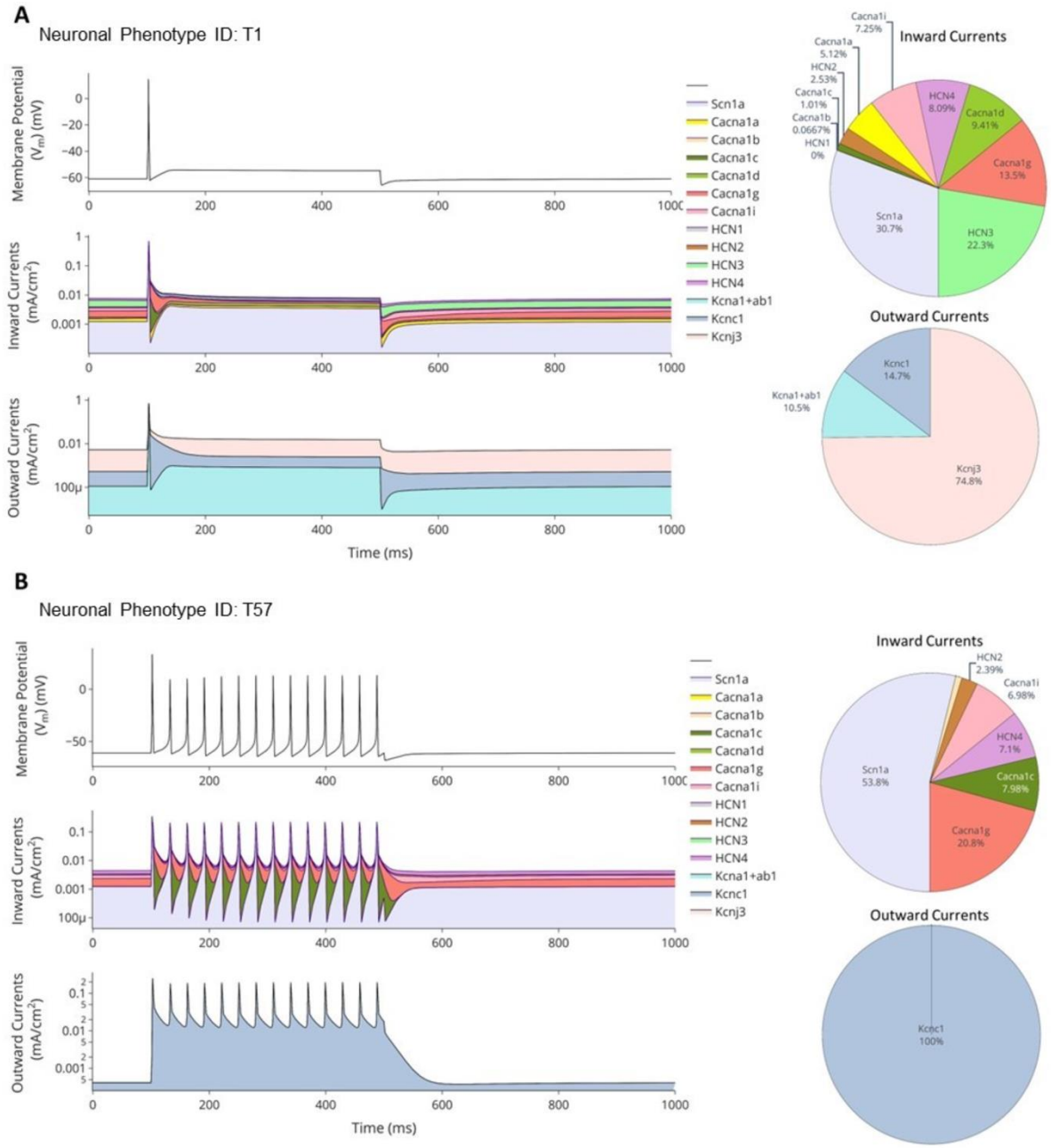

Figure S5: Currentscapes that depict dynamic contribution of ionic currents that underly a representative phasic (T1) and tonic (T57) firing profiles at 0.2 nA current clamp stimulus. Membrane potential is shown in the topmost panel, with the contribution of inward ionic currents and outward ionic currents in the next two panels, plotted on a semi-logarithmic scale. Overall percent contribution of inward and outward ionic currents is depicted as a pie chart shown alongside the currentscapes. The currentscapes revealed that *Scn1a* (Nav 1.1) contributes the most to inward currents in both neuronal-types, where it contributes to 53.8% of inward currents in tonically firing T57 and 30.7% of inward currents in phasically

firing T1. In both T1 and T57, *Cacna1g* (Cav 3.1) and *Cacna1d* (Cav 1.3) sustained the depolarized membrane potential. The difference in neuronal behavior between the phasically firing T1 and tonically firing T57 is seen largely in the outward currents. *Kcnj3* (Kir 3.1) contributes to 74.8% of outward currents in phasically firing T1, whereas outward currents in tonically firing types are primarily due to *Kcnc1* (Kv 3.1).

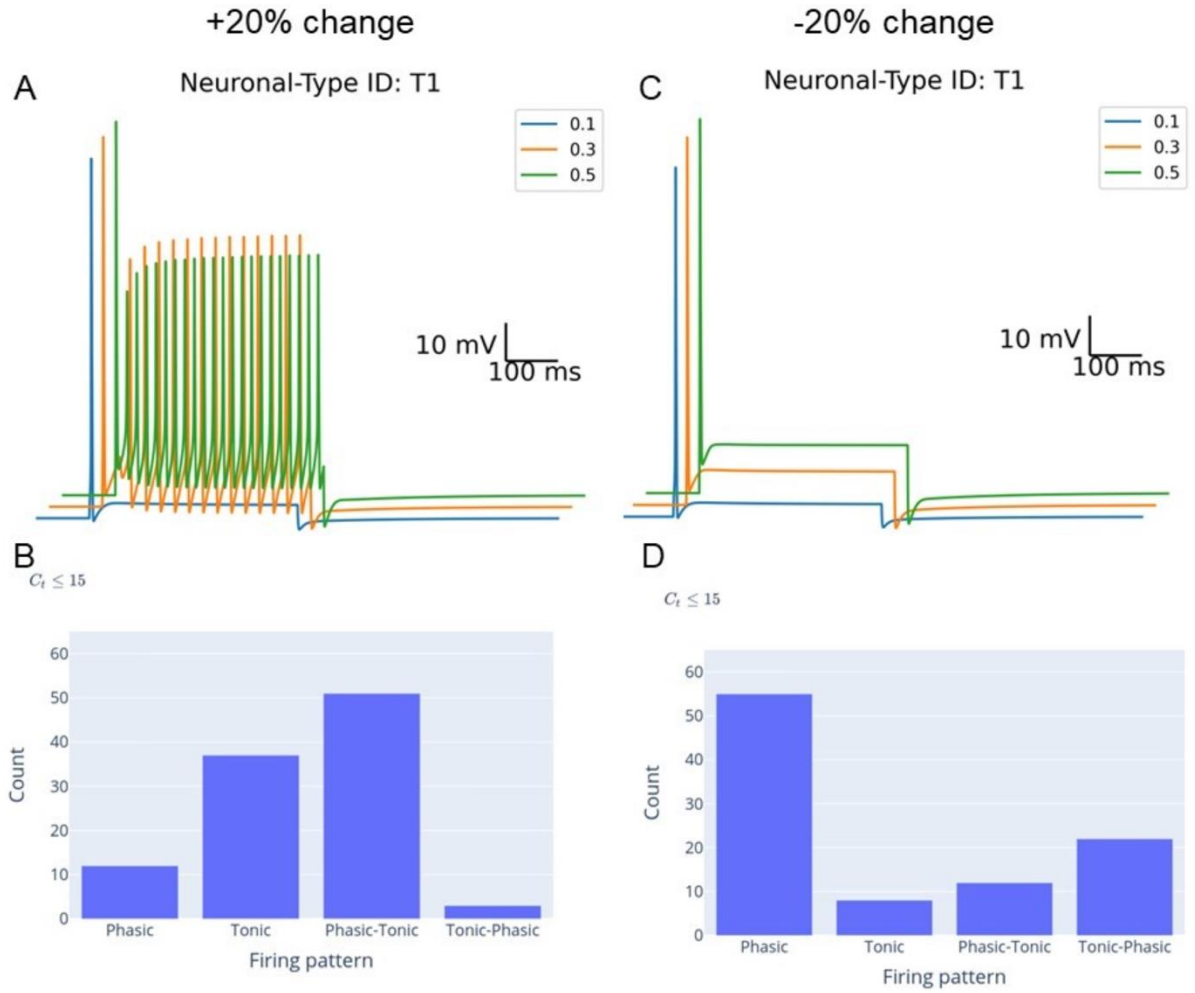

Figure S6: Effect of varying the Na^+ channel inactivation parameter (h_∞) on electrophysiological behavior. Simulations are shown for a +20% change in h_∞ (A and B) and a -20% change in h_∞ (C and D). A C_t threshold of 15 was used so that results for the electrophysiological behavior of neuronal phenotype T1 can be compared to the results in Figure 4, which shows that T1 has phasic behavior at all three stimulus intensities. h_∞ values ranged within the range of what would be expected for inter-model variability.

Reviewer 2

The study is motivated by a fascinating idea, which is, being able to explicitly include information about patterns of ion channel expression into an excitable membrane model, in this case, from intrinsic cardiac neuron transcriptomics. However, the models were chosen from databases that assume channel dynamics, in particular gating dynamics, that by their formulation bias the predictions in at least a couple of ways. The most important one is the use of powers in the gating terms, which impact the sizes of the maximal conductances of the model. One key question that arises from this is: are the ratios of Na and K maximal conductances equivalent to the ratios of the levels of expression from the data corresponding to Na and K channels? The models chosen for the study, as presented, predict ratios of 3-5 times as many Nav1.1 channels as Kv1.1 channels, for instance. Is this accurate? I would very much like to see some evidence to that effect. Electrophysiological recordings and other splice variant data indicate the opposite (several fold more K channels in comparison to Na channels, for instance), but that is not conclusive data that applies to all species and neurons within them.

Regarding originality, the question has been asked before (e.g. Herrera-Valdez, et al. 2013, Nowotny et al. 2007), but to my knowledge, there have not been any studies in which transcriptomic or proteomic data have been used. In this regard, the study is motivated by a very interesting paradigm linking modelling and experimental measurements, but again, choose arbitrarily from model databases arguing that many people use those models (see comments about powers in gating terms in annotated pdfs and above). One important fact to consider is that the behaviour of the neurons of interest in the study can be captured initially with a simple 2D model with voltage-gated Na and K-delayed rectifier channels. The conclusions from using a model with high dimensionality are hard to interpret and it is easy to conclude, wrongly, that "wild combinations of parameters indicate wild combinations of expression levels", as suggested by some. Highly dimensional models may show combinations of parameters that may not be correct in light of physiological considerations. Also, the authors choose to model ionic currents with different functional forms (fundamentally different assumptions for the underlying biophysics) within the same model, which does not help for interpretation.

As to the dynamics of the model, since there seems to be a gradient of behaviours that stem all from phenomena captured by 2D biophysics, I think the authors could have focused on building up from simple models to tackle the issues of diversity in the neuronal population, to network dynamics as mentioned in the discussion of the paper. The model does not go significantly further in making predictions, in comparison to the transcriptomics data, but analysing the dynamics from a tractable perspective would have been more informative, and then the inclusion of more ion channels to explain how redundancies occur would have been appropriate.

In spite of the poor modelling and choices, and having done no geometrical or other kinds of analysis that are more meaningful than the statistics, I believe that the approach heads fundamentally in the right direction, and other modelling approaches could complement what is reported in this study, provided that the transcriptomic data is shared properly (not just the binary data about whether a channel gene is transcribed or not).

***Response**:*
We appreciate the detailed insight and critical feedback to improve the manuscript and address the critiques as below. We agree that the strength of this work lies in exploring the premise that transcriptomic data on ion channel expression can explicitly be included in an excitable membrane model. We have addressed the reviewer's major concerns stated in the above paragraphs in the section below and address each piece of specific feedback after.

We agree with the reviewer's concern regarding how gating parameter powers can influence ion channel dynamics and electrophysiological firing patterns.

***Action Taken**:*
We have added an explanation of our rationale for choosing Hodgkin-Huxley models in the Discussion section. The text starts with: "The models were selected from three public databases: Channelpedia (Ranjan et al., 2011), ModelDB (McDougal et al., 2017), and Ion Channel Genealogy (Podlaski et al., 2017)... may be used without any loss of general function."

***Response**:*
We have addressed the reviewer's concern about the ratio of Na and K channels by including an analysis showing that the relative expression of Na:K is 3.4 on average compared to the 4.2-fold difference in conductance values predicted by the model.

***Action Taken**:*
We have included a short discussion of the limited protein expression data available, which indicates that Na channel expression is higher than K channel expression. This can be found in the Discussion section.

***Response**:*
The shortlisted ion channels from the databases were further screened by comparing their activation and inactivation kinetics (mh curves).

***Action Taken**:*
We have added the following sentence in the Methods section: "Multiple ion channel models of the same genotype, mined from the different databases, were compared on the basis of their activation and inactivation dynamics to assess their regions of operation."
In addition to selecting Na and K models that were already part of the Methods section, we have added a paragraph on how voltage-gated Ca channels were shortlisted. We have expanded Figure 4 to demonstrate the mh curves for all the voltage-gated sodium and calcium channels explored.

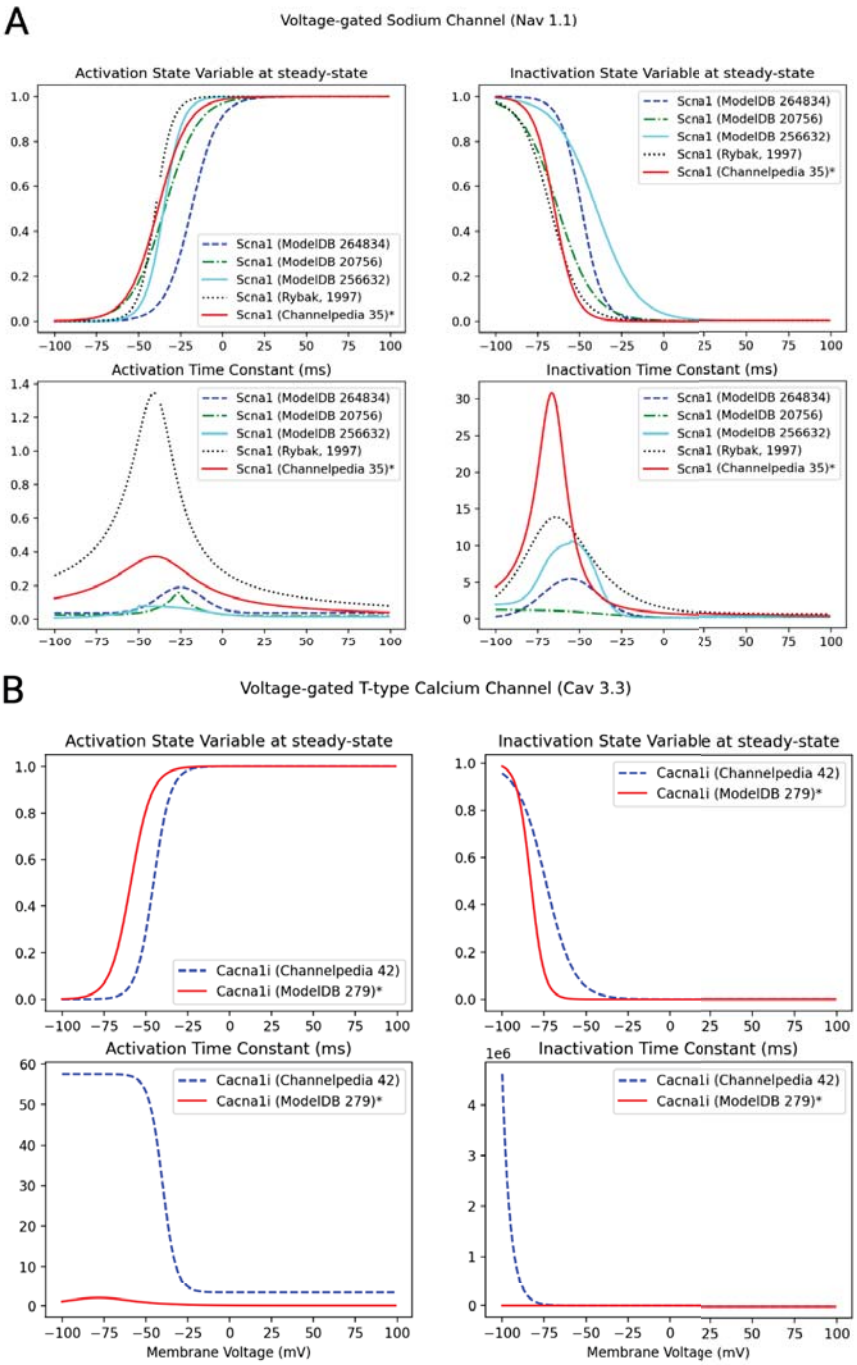

Response:

The reviewer makes a good point about the high dimensionality of the model making it more difficult to interpret the results. Our study addresses this directly by showing that variability in the combinations of ion channels converges at the physiological scale to yield lower dimensionality of phenotypes (as defined by a particular response to stimulus). Regarding the concern about high dimensional models containing parameters that may be unphysiological, the relative conductances used in the model were correlated with the relative expression levels in the

transcriptomic data. An analysis of the correlation between relative conductance and relative expression was performed as result of reviewer feedback (thanks!). We would like to note that transcriptomic data were not used to constrain the parameter values. The analysis showed that model parameter values correspond with physiological measurements.

Action Taken:
This analysis was added as Figure 8 in the revised manuscript.

Response: *We agree with the reviewer that we have employed different functional forms of the calcium channel model. Our understanding is that each variant of calcium channels has a distinct and unique gating property. These channels differ with respect to their threshold of activation and speed of activation. Additionally, not all variants inactivate, and if they do, do not inactivate to the same extent and by the same gating variable. Owing to this variability, a single functional form could not be employed for all calcium channels.*

Action Taken: *In the manuscript, we have explicitly mentioned how we attempted to ensure biophysical viability of the calcium models chosen in the Methods and Discussion.*

Response:
The reviewer makes an excellent point that an alternative to our approach of simulating all of the ion channels found in the transcriptomic data would have been to start from a two ion channel model and progressively add channels to explain how channel redundancies occur. We believe that both approaches are rigorous and informative. We opted for simulating all of the ion channels together because the neuronal genotype with the fewest ion channels has one sodium and one potassium channel. About 38% of our neuronal genotypes exhibited a firing pattern that was invariant to parametric variations. Due to this emergent difference in response to parametric variations, exploring a mosaic of ion channel combinations across the 104 neuronal genotypes was more appropriate to survey the range of physiological firing patterns, as depicted in Figure 5. Restricting our neuronal-genotype to 2 ion channel models (T104) would result in a consistent phasic firing pattern which would be representative of 38% of the entire neuronal cohort. By comparing the firing behaviour of different neuronal genotypes, we are able to examine ion channel redundancies.

Action Taken: *We have added a sentence at the end of the introduction acknowledging this alternative way to frame the manuscript as an equally valid alternative.*

Response:
Thank you for pointing out that we did not include a link to the original transcriptomic dataset used for model development. The transcriptomic data are available on the SPARC portal (https://doi.org/10.26275/z6jn-j5tx).

Action Taken: *A sentence directing the reader to this resource has been added to the Data and code availability subsection in the Methods.*

Specific comments

Highlighted manuscript text*:* The parameters of the ion channel models were grounded based on passive properties: resting membrane potential, input impedance, and rheobase

Comment*:* What do passive properties have to do with the active properties coferred by the channels?

Response: *The reviewer is correct in pointing out that the passive properties are not directly related to the active properties conferred by the channels. We constrained the model based on these passive properties because we did not want to bias our result or overfit the model in any way.*

Action Taken: *We now clarify this in the Abstract. "The parameters of the ion channel models were grounded based on passive properties (resting membrane potential, input impedance, and rheobase) to avoid biasing the dynamic behaviour of the model."*

Highlighted manuscript text: The single-cell transcriptomic data formed the basis for ion channel combinations in each neuronal model

Comment: How? What is the direct relationship between the transcriptomic data and the ion channel combinations in the model?

Response and Action Taken: *We have clarified this bullet point to add more information on the relationship between the transcriptomic data and the ion channel combinations. The bullet point now reads: "The single-cell transcriptomic data were thresholded to select the ion channel combinations in each neuronal model".*

Highlighted manuscript text: Heterogeneity in the electrophysiological behavior of neurons is driven by variation in ion channel expression

Comment: This is obvious without the model. What are the patterns or mechanisms underlying the heterogeneity as explained by the model?

Response: *The reviewer is correct that this statement is obvious without the model.*

Action Taken: *We have replaced the bullet point with a new one highlighting a result that was spurred by reviewer feedback. The new bullet point is: "The ratios of model-predicted conductance values are correlated with the gene expression ratios from transcriptomic data."*

Highlighted manuscript text: we use the well-established Hodgkin-Huxley models and combine them with single-cell transcriptomics data to identify specific ion channel combinations for each neuron

Comment: These models are well known for not being able to reproduce firing patterns in neurons with accuracy in regard to ion channel expression or ion current data. Part of the problem is the powers in the gating, which cause the values of the maximal conductances to missrepresent the sizes of the ion channel populations. Also, the model used in this paper has a multitude of functional forms for different ion channels, all voltage-gated or ligand-gated, which introduces an unwanted source of variability.

Response: *This is a fair point that there are certainly limitations that come with using Hodgkin-Huxley models. We found that in our case we were able to reproduce reasonable firing patterns with correlations between ion channel expression and model conductances. The maximal ion channel conductances were selected based on what values produced reasonable resting membrane potential, input impedance, rheobase, and leak reversal potential. We found that the model-predicted conductances were correlated to the ion channel expression level, which was not used to select model conductances. Furthermore, other ion channel conductances predicted by models tuned to electrophysiological data have been found to be correlated with ion channel expression levels (Nandi et al., 2022).*

Action Taken*: An additional figure (Fig. 8) has been added to address this point (see responses to similar comments below for more details and figure). We have also additionally explained the pecking order of the public databases and our approach at initial screening of the models available.*

Highlighted manuscript text: neurons of the same cell type have electrophysiological behavior consistent with each other in response to current clamp stimulus, but vary in their ion channel conductance densities

Comment: Please provide evidence for this statement in the context of this paper.

Response: *This sentence paraphrases a point made in Goaillard and Marder 2021, about how neurons of the same cell type have variability in ion channel conductance densities while showing similar behavior. In the context of our work, ICN neurons have been shown to be electrically excitable with phasic or tonic responses (McAllen et al., 2011). Our transcriptomic data combined with the models indicate that there are many combinations of ion channels that lead to phasic behaviour and many combinations that lead to tonic behaviour.*

Action Taken: *We have added a reference to this sentence.*

Highlighted manuscript text: Goaillard & Marder, 2021

Comment: Yes, but see Nowotni, 2007. Tails wagging the dogs ([PDF] mit.edu)

Response: *We stated that ion channel heterogeneity may contribute to the observation that neurons of cell type can have consistent electrophysiological behavior in response to one stimulus but a variety of responses in response to a different input (Goaillard & Marder, 2021). If we understand correctly, the reviewer is saying that rather than ion channel heterogeneity, the phasic versus tonic behaviour are a result of bifurcations in the stability of the dynamical system (Nowotny & Rabinovich, 2007).*

We agree with the reviewer's viewpoint. There have been instances where a parameter shift in single-neuronal Hodgkin-Huxley model has resulted in varied firing characteristics (Guckenheimer & Labouriau, 1993; Rush & Rinzel, 1995; Izhikevich, 2003; Doi & Kumagai, 2005; Postnova et al., 2007)). We have observed 64/104 of our neuronal genotypes models to exhibit both tonic and phasic firing based on stimulus strength and ion channel conductances.

However, the firing characteristics of single-neurons are rapidly adjusted when in a network. In their model, Nowotny states that the "transformations of the phase portrait depend only on one control parameter, i.e., the equal strength of the couplings". In vivo, the principal neurons form a network within the RAGP wherein the 64/104 phasic and tonic neurons will interconnect with the 40/104 robustly phasic neurons, and non-excitable small intensely fluorescent cells (Hanna et al., 2021; Moss et al., 2021). The individual firing characteristics of these single neurons will thereby be mediated by the strength of their connections as well as the inputs received from vagus nerve. While the strength of the couplings does not apply for single-neuron models (Nowotny & Rabinovich, 2007), a bifurcation analysis framework may be more effective as we extend this work to examine our principal neuron models in a network.

Action Taken: *We have added information on bifurcation analysis of the planned network model as part of the Discussion, starting with "Several planned extensions of the current model…."*

Highlighted manuscript text: We present a strategy for using single-neuron transcriptomic data to predict neuronal membrane physiology, demonstrating a workflow for building a library of neuronal phenotype models

Comment: This is extremely interesting. However, do you really match the relative ratios of pair-wise ion channel expression with the dynamics in the model and the corresponding pair-wise ratios of maximal conductances corresponding to those ion channels?

Response: *This is a very interesting point that we had not fully considered in the manner you suggest, and we thank you for bringing it up.*

Action Taken: *We calculated the median expression fold differences compared to Cacna1a, the ion channel with the lowest conductance in the model. The median fold difference was calculated after normalizing all gene expression using the housekeeping gene GAPDH (ΔCt).*

The fold difference for each gene compared to Cacna1a was calculated ($\Delta\Delta Ct = \Delta Ct_{gene} - \Delta Ct_{Cacna1a}$), then used to calculate fold difference in expression. The model-predicted ratio of conductances were correlated with the ratio of expression levels in the transcriptomic data (R^2=0.67). There are some exceptions to the correlation, notably Hcn3 and Cacna1b which were removed for the correlation analysis. It should be noted that the maximal conductance values were selected based on the passive electrical properties of the neurons, not the transcriptomic data. Taken together, these findings suggest that the model predicted conductances independently correlate with relative expression of ion channels. The figure below (Fig. 8 in the manuscript) and additional text discussing the correlation between the expression and conductance values have been added to the results section.

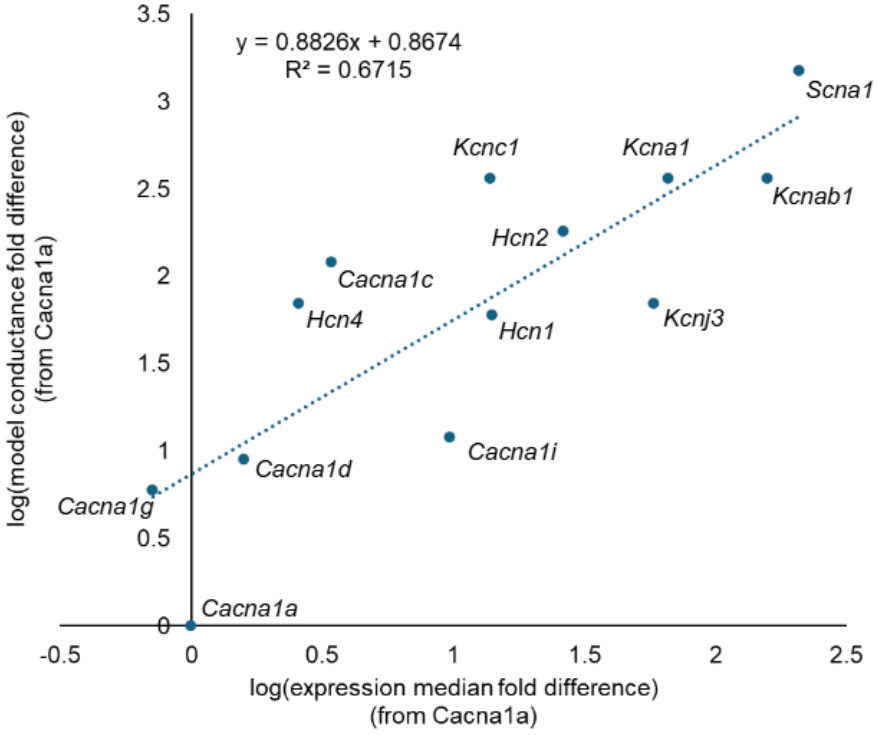

Highlighted manuscript text: *used the Goldman-Hodgkin–Katz*

Comment: Why is this a good idea for Ca channels and not for Na or K voltage-gated channels? They all gate with voltage and they all conduct ions…
The nonlinear contributions from the driving force terms in the GHK model can differ greatly from other ion-channel contributions, shifting the balance between channels predicted by the model.

Response: *We agree with the reviewer's comment that the GHK equation applies to Ca, Na and K voltage-gated channels. Intra and extracellular potassium and sodium concentrations are tightly regulated during a spike such that they are maintained within the same order of magnitude, which results in their Nernst Potentials to remain constant. On the other hand, intracellular calcium concentration rises ~10-fold during a spike. Extracellular calcium*

concentration is of the order of mM, while basal intracellular calcium concentration is of the order of 100s nM. Calcium transient, which underlies an action potential, causes intracellular calcium concentration to rise to the order of µM, which results in a ~30 mV change in its Nernst Potential. To ensure that this change in electrochemical driving force is accounted for in our models, we explicitly incorporated the GHK model for Ca channels.

Action Taken: *We have added this explanation in the Methods section.*

Highlighted manuscript text: *We refer to each unique combination of ion channels as a neuronal phenotype.*

Comment: Not necessarily accurate in the sense that similar electrophysiological or otherwise behaviours could be displayed by neurons having the same “electrophysiological phenotype”

Response: *You are correct, neuronal genotype would be more accurate for what we are describing.*

Action Taken: *We have changed this nomenclature throughout the manuscript.*

Highlighted manuscript text: *Kcna1 (Kv 1.1) is a delayed rectifier potassium (KDR) channel, which is non- or slowly-inactivating (timescale of seconds) (Song, 2002). Our data set showed robust expression of Kcna1 (.. subunit of Kv 1.1). There was also a dominant expression of Kcnab1 (ß1 regulatory subunit) across all neuronal phenotypes*

Comment: What is the range of ratios of Nav1.1 to Kv1.1 channels in the neurons? Is it larger than 1? What are the corresponding ratios of maximal conductances in the corresponding neurons? if those two quantitites do not match, the approach is flawed at some point. My guess would be the choice of models.

Response:
Using the same methodology as previously described to calculate relative expression levels, we found that the Scn1a was expressed on average at 3.4 (median 2.7) times greater levels than Kcna1 in each of the neurons. This ratio is in agreement with the maximal conductance ratio for Nav1.1 and Kv1.1, which was 4.2.

On the protein expression side, there is limited data that suggests Nav1.1 expression is about 1.4 times greater than Kv1.1 expression (Gu et al., 2018). These findings are from mammalian central neurons, as measurements in mammalian peripheral neurons could not be found. Furthermore, single channel conductance for Nav1.1 is roughly 1.5 times higher than Kv1.1 (17 pS for Nav1.1 compared to 12 pS for Kv1.1) (Vanoye et al., 2006; Streit et al., 2014). Thus, the combination of 1.4 fold expression and 1.5 fold channel conductance results in an

approximately 2 fold higher conductance for Nav1.1. These data also suggest that our conductance ratio for Nav1.1 and Kv1.1 is reasonable.

Action Taken:
Information on the relative conductance ratios is included in the results section in the text corresponding to Figure 8. The literature on protein expression of Nav1.1 versus Kv1.1 has been added to the Discussion section.

Highlighted manuscript text: *degenerate parameter set*

Comment: what made those parameter sets degenerate?

Response: *The reviewer is correct in pointing out that just because these parameter sets had physiologically reasonable input impedance, reversal potential, and rheobase doesn't mean they are degenerate.*

Action Taken: *The label degenerate has been removed.*

Highlighted manuscript text: F*igure 5 comment (currently Fig. 7 in the manuscript)*

Comment: Show an enhancement of the curve for the range before 0.1 nA in the same or in a different graph

Response and Action Taken: *We have added this inset to the figure.*

Comment: The models chosen for this study have one big flaw. The prediction of the number of Nav channels is going to be affected heavily by the powers in the gating terms. This is an inherited feature from the HH model but it can be corrected. Is it really the case that the expression of Nav1.1 channels in a single neuron is 3-4 times the expression of Kv1.1 channels, and not the opposite?

Response: *As mentioned in the previous response, the qPCR data and protein data support this model prediction. It has been reported that Nav1.1 expression is higher than Kv1.1 expression (Gu et al., 2018). The qPCR data show that the mean Scn1a expression was 3.4 times higher than Kcna1 expression on a cell by cell basis. The minimum expression ratio was 1.4 and the maximum was 50.4. This expression ratio and corresponding maximal conductance ratio was not surprising to us given that similar ratios of maximal conductances for sodium and*

KDR channels have been reported previously (Rybak et al., 1997; Rogers et al., 2000; Yaghini Bonabi et al., 2014).

***Action Taken:** Additional text addressing these concerns has been added to the Discussion section in the "Strengths and limitations of the model" subsection.*

Comment: The discussion in lines 446-464 approximately is highly relevant to the observations made above in regard to the sizes of the maximal conductances. However, even if the assumptions for the gating parameters were justified, the powers and their effect on the gating variables yield radically different predictions about the Na/K complements of channels.

***Response:** As stated in the lines of the Discussion section highlighted, we agree that there are limitations to translating transcriptomic data to electrophysiological dynamics.*

***Action Taken:** We have expanded upon the Discussion section to include text on the available protein data that suggest that Nav1.1 expression may be higher than Kv1.1 expression. We also added text on how the translation of ion channel expression levels to channel dynamics is further complicated by the different single channel conductances of different ion channels.*

References

Doi S & Kumagai S (2005). Generation of very slow neuronal rhythms and chaos near the Hopf bifurcation in single neuron models. *J Comput Neurosci* **19,** 325–356.

Goaillard J-M & Marder E (2021). Ion Channel Degeneracy, Variability, and Covariation in Neuron and Circuit Resilience. *Annu Rev Neurosci* **44,** 335–357.

Guckenheimer J & Labouriau JS (1993). Bifurcation of the Hodgkin and Huxley equations: A new twist. *Bull Math Biol* **55,** 937–952.

Gu Y, Servello D, Han Z, Lalchandani RR, Ding JB, Huang K & Gu C (2018). Balanced activity between Kv3 and Nav channels determines fast-spiking in mammalian central neurons. *iScience* **9,** 120–137.

Hanna P et al. (2021). Innervation and Neuronal Control of the Mammalian Sinoatrial Node a Comprehensive Atlas. *Circ Res* **128,** 1279–1296.

Izhikevich EM (2003). Simple model of spiking neurons. *IEEE Trans Neural Netw* **14,** 1569–1572.

McAllen RM, Salo LM, Paton JFR & Pickering AE (2011). Processing of central and reflex vagal drives by rat cardiac ganglion neurones: an intracellular analysis. *J Physiol* **589,** 5801–5818.

Moss A, Robbins S, Achanta S, Kuttippurathu L, Turick S, Nieves S, Hanna P, Smith EH, Hoover DB, Chen J, Cheng ZJ, Ardell JL, Shivkumar K, Schwaber JS & Vadigepalli R (2021). A single cell transcriptomics map of paracrine networks in the intrinsic cardiac nervous system. *iScience* **24,** 102713.

Nandi A, Chartrand T, Van Geit W, Buchin A, Yao Z, Lee SY, Wei Y, Kalmbach B, Lee B, Lein E, Berg J, Sümbül U, Koch C, Tasic B & Anastassiou CA (2022). Single-neuron models linking electrophysiology, morphology, and transcriptomics across cortical cell types. *Cell Rep* **40,** 111176.

Nowotny T & Rabinovich MI (2007). Dynamical origin of independent spiking and bursting activity in neural microcircuits. *Phys Rev Lett* **98,** 128106.

Postnova S, Voigt K & Braun HA (2007). Neural synchronization at tonic-to-bursting transitions. *J Biol Phys* **33,** 129–143.

Rogers RF, Rybak IA & Schwaber JS (2000). Computational modeling of the baroreflex arc: nucleus tractus solitarius. *Brain Res Bull* **51,** 139–150.

Rush ME & Rinzel J (1995). The potassium A-current, low firing rates and rebound excitation in Hodgkin-Huxley models. *Bull Math Biol* **57,** 899–929.

Rybak IA, Paton JFR & Schwaber JS (1997). Modeling Neural Mechanisms for Genesis of Respiratory Rhythm and Pattern. I. Models of Respiratory Neurons. *J Neurophysiol* **77,** 1994–2006.

Streit AK, Matschke LA, Dolga AM, Rinné S & Decher N (2014). RNA editing in the central cavity as a mechanism to regulate surface expression of the voltage-gated potassium

channel Kv1.1. *J Biol Chem* **289,** 26762–26771.

Vanoye CG, Lossin C, Rhodes TH & George AL Jr (2006). Single-channel properties of human NaV1.1 and mechanism of channel dysfunction in SCN1A-associated epilepsy. *J Gen Physiol* **127,** 1–14.

Yaghini Bonabi S, Asgharian H, Safari S & Nili Ahmadabadi M (2014). FPGA implementation of a biological neural network based on the Hodgkin-Huxley neuron model. *Front Neurosci* **8,** 379.

Dear Professor Vadigepalli,

Re: JP-RP-2024-287595R1 "Biophysical Modelling of Intrinsic Cardiac Nervous System Neuronal Electrophysiology based on Single-cell Transcriptomics" by Suranjana Gupta, Michelle M Gee, Adam John Hunter Newton, Lakshmi Kuttippurathu, Alison Moss, John D. Tompkins, James S Schwaber, Rajanikanth Vadigepalli, and William Lytton

We are pleased to tell you that your paper has been accepted for publication in The Journal of Physiology.

The last Word (or similar) version of the manuscript provided will be used by the Production Editor to prepare your proof. When this is ready you will receive an email containing a link to Wiley's Online Proofing System. The proof should be thoroughly checked and corrected as promptly as possible.

Authors should note that it is too late at this point to offer corrections prior to proofreading. Major corrections at proof stage, such as changes to figures, will be referred to the Editors for approval before they can be incorporated. Only minor changes, such as to style and consistency, should be made at proof stage. Changes that need to be made after proof stage will usually require a formal correction notice.

All queries at proof stage should be sent to: TJP@wiley.com.

Following copyediting and typesetting the accepted version will be published online.

Yours sincerely,

Natalia Trayanova
Senior Editor
The Journal of Physiology

IMPORTANT POINTS TO NOTE FOLLOWING YOUR PAPER'S ACCEPTANCE:

If you would like to receive our 'Research Roundup', a monthly newsletter highlighting the cutting-edge research published in The Physiological Society's family of journals (The Journal of Physiology, Experimental Physiology, Physiological Reports, The Journal of Nutritional Physiology and The Journal of Precision Medicine: Health and Disease), please click this link, fill in your name and email address and select 'Research Roundup':
https://www.physoc.org/journals-and-media/membernews

• TRANSPARENT PEER REVIEW POLICY: To improve the transparency of its peer review process, The Journal of Physiology publishes online as supporting information the peer review history of all articles accepted for publication. Readers will have access to decision letters, including Editors' comments and referee reports, for each version of the manuscript as well as any author responses to peer review comments. Referees can decide whether or not they wish to be named on the peer review history document.

• You can help your research get the attention it deserves! Check out Wiley's free Promotion Guide for best-practice recommendations for promoting your work at: www.wileyauthors.com/eeo/guide. You can learn more about Wiley Editing Services which offers professional video, design, and writing services to create shareable video abstracts, infographics, conference posters, lay summaries, and research news stories for your research at: www.wileyauthors.com/eeo/promotion.

• IMPORTANT NOTICE ABOUT OPEN ACCESS: To assist authors whose funding agencies mandate public access to published research findings sooner than 12 months after publication, The Journal of Physiology allows authors to pay an Open Access (OA) fee to have their papers made freely available immediately on publication.

The Corresponding Author will receive an email from Wiley with details on how to register or log-in to Wiley Authors Services where you will be able to place an order.

• You can check if your funder or institution has a Wiley Open Access Account here: https://authorservices.wiley.com/author-resources/Journal-Authors/licensing-and-open-access/open-access/author-compliance-tool.html.

EDITOR COMMENTS

Reviewing Editor:

Thank you for thoroughly addressing the critiques.
